Available online at www.sciencedirect.com
ScienceDirect
Journal of Sound and Vibration 318 (2008) 1154–1179
JOURNAL OF SOUND AND VIBRATION
www.elsevier.com/locate/jsvi

On lateral response of structures containing a cylindrical liquid tank under the effect of fluid/structure resonances

N.K.A. Attari, F.R. Rofooei*

Civil Engineering Department, Sharif University of Technology, Tehran, Iran

Received 7 January 2008; received in revised form 25 April 2008; accepted 1 May 2008
Handling Editor: C.L. Morfey
Available online 24 June 2008

Abstract

The lateral response of a single degree of freedom (SDOF) structural system containing a rigid circular cylindrical liquid tank, under harmonic and earthquake excitations is considered. The governing differential equations of motion for the combined system is derived considering the first 3 liquid sloshing modes (1,1), (0,1), and (2,1), under horizontal excitation. The system is considered nonlinear due to the convective term of liquid acceleration and the nonlinear surface boundary conditions, both caused by the inertial nonlinearity. The harmonic and seismic response of the system is investigated in the neighborhood of 1:1 and 1:2 internal resonances between the SDOF system and the first asymmetric sloshing mode. These resonance cases can be regarded as autoparametric if an internal resonance exists between the sloshing mode (1,1) and the structural system, while the frequency of the external harmonic excitation is tuned to the system's structural frequency. In addition, the effect of system's horizontal and vertical displacement on lateral components of acceleration as well as the effect of sloshing wave amplitude on liquid-induced dynamic pressure is investigated. The numerical results illustrates the efficiency of the liquid sloshing modes in reducing the seismic response of the structural system to a large extent, particularly when the fundamental frequency of the system is close to the dominant frequency of the earthquake record. Also, the increase in the Fourier amplitudes of the sloshing modes is an indication of energy transfer from structure to liquid due to nonlinear interaction. Considering 3 sloshing modes shows that the amplitude of asymmetric liquid mode (1,1) in some cases becomes smaller in comparison to the case with 1 mode, and the other sloshing modes absorb part of the energy imparted from the SDOF system.

1. Introduction

The concept of using sloshing-induced hydrodynamic forces to control structural vibration has long been recognized. It is known that shallow liquid in a container experiences traveling sloshing waves. Increasing the depth of the liquid will transform them into a standing sloshing wave that vibrates in its fundamental mode. The efficiency of the tuned liquid dampers (TLD) that use shallow liquid to perform, in controlling the lateral response of structures has been studied analytically, numerically, and experimentally. Applications of TLD in controlling the response of tall buildings were investigated by Chang and Gu [1] and Yamamoto and

*Corresponding author. Tel./fax: +98 21 66164233.
E-mail addresses: nattary@alum.sharif.edu (N.K.A. Attari), Rofooei@sharif.edu (F.R. Rofooei).

0022-460X/$ - see front matter © 2008 Elsevier Ltd. All rights reserved.
doi:10.1016/j.jsv.2008.05.007

Kawahara [2]. Modi and Munshi [3] used a barrier for increasing the energy dissipation in a rectangular TLD system. Fujino et al. [4] developed a model for rectangular TLD subjected to horizontal excitation using shallow water wave theory. However, most of these studies did not recognize the nonlinear interaction between the liquid and the supporting structure [5,6].

Dynamic response of elastic structural systems carrying liquid storage tanks has been extensively explored during the last few decades. Shepherd [7] investigated the behavior of elevated water tanks under seismic excitation. Ibrahim et al. examined the nonlinear interaction in elevated water tanks subjected to vertical and horizontal sinusoidal ground motions in the neighborhood of internal resonances [8–12]. They showed that the liquid sloshing modes and the vibrational modes of the elastic supporting structure were coupled through inertial nonlinearity.

The inertial nonlinearity can be generated through the presence of concentrated or distributed masses. Nonlinearity may appear in the governing partial differential equations of motion or in boundary conditions or both. The free surface condition in liquids is considered to be a nonlinear boundary condition [13,14], as well as the acceleration of the liquid particles that includes a nonlinear convective term.

Inertial nonlinearity could lead to internal resonance condition among the interacting modes when $\sum_{j=1}^{n} k_j \omega_j = 0$, in which k_j is an integer and ω_j is the jth natural frequency of the coupled modes. Setting the frequency of the external excitation equal to the fundamental frequency of the system (primary resonance) causes the forced structural response under the external excitation to act as a parametric excitation for the liquid. This is due to the coupling between the system's displacement and the liquid sloshing modes. This type of coupling is referred to as autoparametric resonance. Ibrahim et al. [10] showed that in the vertical motion of a system (elevated water tank) under parametric resonance of the first normal mode, the system response have the characteristics of a hard nonlinear system. But, when the second normal mode is parametrically excited, the system behaves as a soft nonlinear model. They also showed that at combination resonances, the equivalent linearized system is parametrically stable. Ibrahim and Li [11] observed that when the first normal mode of the system is externally excited in horizontal direction, the system performs as a nonlinear soft model with weak autoparametric resonance.

Different types of nonlinear interactions could exist for a liquid tank standing on an elastic structure. They include the interaction of the liquid sloshing modes with the breathing and flexural modes of the tank [15–17], the interaction between two sloshing modes [18,19], the interaction between tank's breathing and flexural modes [20], and the interaction of the liquid sloshing modes with the modes of supporting elastic structure [8–12,21,22].

Ikeda and Nakagawa [23] considered the nonlinear interaction of the liquid sloshing in rectangular tanks with a supporting elastic structure under horizontal excitation. They showed that for an elastic structure carrying a rigid rectangular tank under vertical sinusoidal excitation, the frequency response curves vary from soft to hard as the tank water depth decreases. In a similar study, Ikeda and Ibrahim observed that when the central frequency of the excitation's power spectral density (PSD) is close to the SDOF system's natural frequency, there is an irregular energy transfer between the structure and the liquid's free surface motion [24]. Depending on the PSD of the external excitation, the liquid's free surface experiences zero motion, uncertain motion (intermittency), partially developed motion, and/or fully developed random motion. Considering the excitation frequency as a control parameter, Ikeda and Murakami investigated the influences of the liquid level and a detuning parameter on the theoretical resonance curves. They showed that the frequency response curves depend on the liquid level and a small deviation of the tuning condition may cause amplitude and phase modulated motions and chaotic vibrations [25].

Miles [18] studied the surface waves in cylindrical basin filled with an inviscid fluid. Using a variational approach, he developed a nonlinear model with 3 coupled sloshing modes under harmonic excitation for a system with weakly coupled free oscillation of liquid sloshing modes. Nayfeh [26,27] examined the same model, obtaining the equations of the modal amplitudes of the surface modes. Holmes [28] investigated the case of vertical excitation when the modal sloshing frequencies are in the ratio of 1:2.

Miles and Henderson [19] reviewed some of the studies on parametrically excited surface waves. The interactions of surface waves in circular cylindrical tanks subjected to a parametric harmonic excitation ($\omega_n \approx 2\omega_m$) was considered by Nayfeh. He examined the modal interactions between these modes and determined the periodically and chaotically modulated motions [13,27]. Furthermore, he investigated the 1:2

internal resonance in general systems and showed that for the case of $\omega_n \approx 2\omega_m$ and $\Omega \approx \omega_n$, modal saturation and energy transfer can take place from directly excited mode to the indirectly excited ones [13,29]. A comprehensive literature survey is provided by Ibrahim et al. [30,31] regarding the liquid sloshing dynamics and its application with or without the presence of various resonance cases.

In this study, the nonlinear interaction between a SDOF structural system carrying a circular cylindrical liquid tank and the sloshing modes of the liquid is investigated. The SDOF system can be assumed as an idealization of a multi-degree of freedom (MDOF) structural system considering its fundamental mode of vibration. Response of this model under horizontal harmonic and earthquake excitations is studied using 1 and 3 sloshing modes in the neighborhood of 1:2 and 1:1 internal resonances. Also, the energy transfer from the structural mode to the first unsymmetrical sloshing mode of liquid is investigated for this system.

2. Governing differential equations of motion

An elastic SDOF structural system is considered. A circular cylindrical liquid tank with fluid depth h and radius R is placed on this structure. The liquid is assumed to be irrotational, non-viscous and incompressible. The effect of wave breaking caused by severe excitation is not considered in this study. Also, an equivalent linear viscous damping term is considered in the modal equations of motion of the liquid [30].

The Cartesian (x,y,z) and cylindrical (r,θ,z) systems of coordinates are considered on the free surface of the liquid, as it is shown in Fig. 1. The wave amplitude in any location (r,θ) is represented by η. The tank is assumed to be rigid and the effects of the first 3 sloshing modes of the liquid are taken into account in this study (Fig. 2).

The experimental investigations by Prize and Penny (1952) and Abramson (1965), as well as a number of other analytical studies [21,24,25,30], emphasizes the importance of the liquid primary modes on lateral response of the system. In other words, if the first asymmetric sloshing mode (1,1) be considered as the primary mode being directly or indirectly excited, then the amplitude of the (0,1) and (2,1) sloshing modes become of second order in comparison to the amplitude of first asymmetric mode. Therefore, the remaining modes are at higher orders, and their effect can be neglected in the problem formulation. The orders of the modal amplitudes of the liquid sloshing modes are:

$$\begin{aligned} &\alpha_{11} = O(\eta), \quad \alpha_{01} = O(\eta^2), \quad \alpha_{21} = O(\eta^2), \quad \alpha_{mn} = O(\eta^m) \\ &a_{11} = O(\eta), \quad a_{01} = O(\eta^2), \quad a_{21} = O(\eta^2), \quad a_{mn} = O(\eta^m) \end{aligned} \tag{1}$$

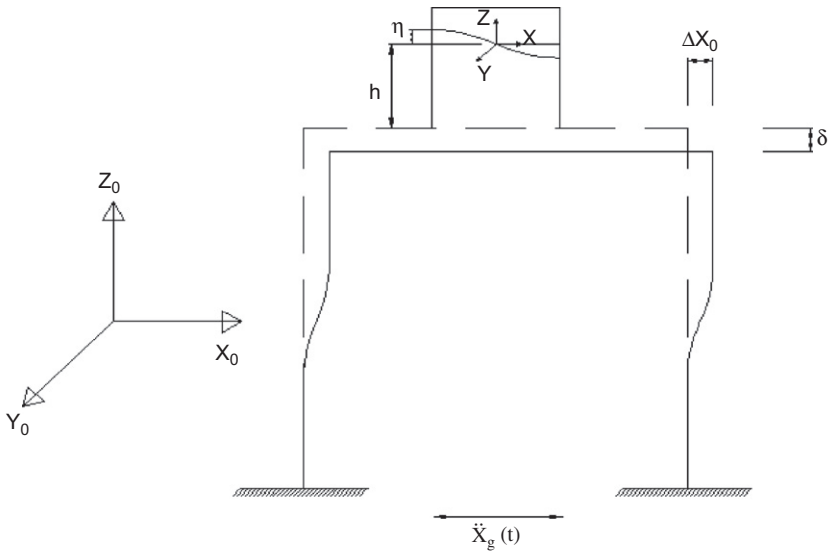

Fig. 1. The SDOF structural system with the cylindrical tank.

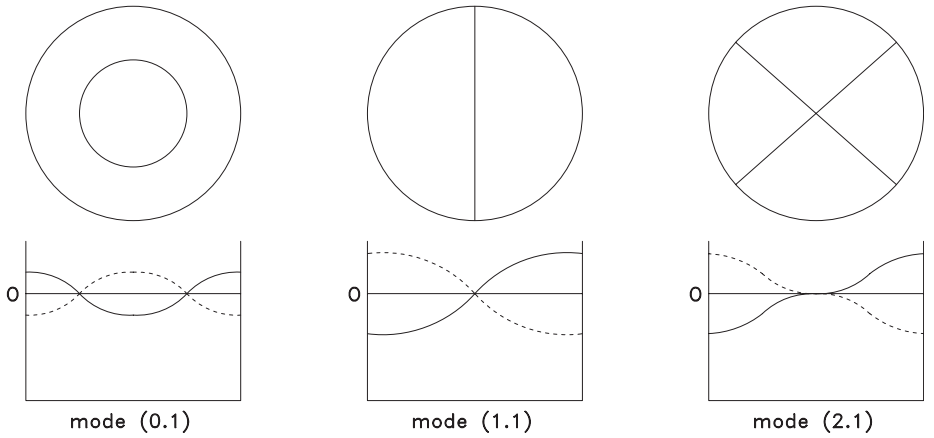

Fig. 2. The 3 sloshing modes considered in the study.

In which, α_{mn} and a_{mn} are the modal amplitudes of the liquid and the velocity potential function, respectively. The (m) and (n) indicate the number of diametric nodal lines and the number of nodal concentric circles, respectively, while η is the liquid wave amplitude. If x_0 denotes the lateral displacement of structure in Cartesian system of coordinates, its polar system of coordinate representation becomes:

$$x_0 = x_0\mathbf{i}_x = x_0 \cos\theta\,\mathbf{i}_r - x_0 \sin\theta\,\mathbf{i}_\theta \tag{2}$$

Then, the velocity of the rigid tank can be expressed as

$$v_0 = \frac{\mathrm{d}x_0}{\mathrm{d}t} = \dot{x}_0 \cos\theta\,\mathbf{i}_r - \dot{x}_0 \sin\theta\,\mathbf{i}_\theta \tag{3}$$

The vertical displacement of the system δ, due to its lateral displacement x_0, is determined as, $\delta = 3x_0^2/5L$, in which L is the structural system's height [12]. Application of the Newton's second law to a liquid particle in a non-viscous liquid leads to:

$$\rho\frac{\mathrm{d}v}{\mathrm{d}t} = -\nabla p + \rho(g - \ddot{\delta}) \tag{4}$$

where ρ, P and v are the liquid's density, pressure and velocity, respectively. The absolute and relative velocities are related through the following equation:

$$\frac{\mathrm{d}v}{\mathrm{d}t} = \frac{\partial v}{\partial t} + v\nabla v \tag{5}$$

The relative velocity of the liquid, $\partial v/\partial t$, is defined in the fixed system of coordinate. The relation between q and v is in the form of:

$$\tfrac{1}{2}\nabla q^2 = v \times (\nabla \times v) + v\nabla v \tag{6}$$

in which $v\nabla v$ is the convective acceleration of the liquid particle moving in the direction of motion with velocity v. This acceleration is measured with respect to the moving system of coordinate of the particles, where the value of q is equal to $q = |v|$. Assuming an irrotational liquid for which $\nabla \times v = 0$, leads to

$$\tfrac{1}{2}\nabla q^2 = v\nabla v \tag{7}$$

Then Eq. (4) becomes

$$\left(\frac{\partial v}{\partial t} + \frac{1}{2}\nabla q^2\right) = -\frac{\nabla P}{\rho} + (g - \ddot{\delta}) \tag{8}$$

If the velocity potential function be defined as $v = \nabla\tilde{\varphi}$, then Eq. (8) may be re-written in the following form:

$$\nabla\left(\frac{\partial\tilde{\varphi}}{\partial t}\right) + \frac{1}{2}\nabla q^2 = -\frac{\nabla p}{\rho} + \nabla(-(g-\ddot{\delta})z) \tag{9}$$

so

$$\nabla\left[\frac{\partial\tilde{\varphi}}{\partial t} + \frac{1}{2}q^2 + \frac{p}{\rho} + (g-\ddot{\delta})z\right] = 0 \tag{10}$$

Integrating Eq. (10) with respect to time gives

$$\frac{\partial\tilde{\varphi}}{\partial t} + \frac{1}{2}\left[\left(\frac{\partial\tilde{\varphi}}{\partial r}\right)^2 + \frac{1}{r^2}\left(\frac{\partial\tilde{\varphi}}{\partial\theta}\right)^2 + \left(\frac{\partial\tilde{\varphi}}{\partial z}\right)^2\right] + \frac{p}{\rho} + (g-\ddot{\delta})z = C_1(t) \tag{11}$$

The velocity potential function, $\tilde{\varphi}$, can be divided into two parts as it is shown in Eq. (12). The first part, φ_0, is related to the tank's motion, while the second part, φ, corresponds to the liquid's relative motion with respect to the tank

$$\tilde{\varphi} = \varphi_0 + \varphi \tag{12}$$

The velocity of the origin O in the coordinate system O-xyz with respect to the fixed coordinate system O′-XYZ can be expressed as

$$v_o = \nabla\varphi_0 = \frac{\partial\varphi}{\partial r}\mathbf{i}_r + \frac{1}{r}\frac{\partial\varphi}{\partial\theta}\mathbf{i}_\theta = \dot{x}_0\cos\theta\,\mathbf{i}_r - \dot{x}_0\sin\theta\,\mathbf{i}_\theta \tag{13}$$

Integrating Eq. (13) and partially differentiating that with respect to the parameter (t) yields:

$$\frac{\partial\varphi}{\partial t} = \ddot{x}_0 r\cos\theta \tag{14}$$

Substituting Eq. (14) into Eq. (11), leads to

$$\frac{\partial\varphi}{\partial t} + \frac{1}{2}\left\{\left(\frac{\partial\varphi}{\partial r}\right)^2 + \frac{1}{r^2}\left(\frac{\partial\varphi}{\partial\theta}\right)^2 + \left(\frac{\partial\varphi}{\partial z}\right)^2\right\} + \frac{p}{\rho} + (g-\ddot{\delta})z + \ddot{x}_0 r\cos\theta = 0 \tag{15}$$

In the above equation, the velocity potential φ is replaced by $\varphi + \int C_1(t)\,\mathrm{d}t$.

The governing differential equation for incompressible liquid is the Laplace equation:

$$\nabla^2\varphi = 0 \Rightarrow \frac{\partial^2\varphi}{\partial r^2} + \frac{1}{r}\frac{\partial\varphi}{\partial r} + \frac{1}{r^2}\frac{\partial^2\varphi}{\partial\theta^2} + \frac{\partial^2\varphi}{\partial z^2} = 0 \tag{16}$$

Also, the differential equation of the motion for the supporting SDOF system under the horizontal ground acceleration $\ddot{x}_g(t)$ becomes

$$\begin{aligned} &m\ddot{x}_0 + c\dot{x}_0 + kx_0 = F_L - m\ddot{x}_g(t) - m\frac{36}{25L^2}x_0(x_0\ddot{x}_0 + \dot{x}_0^2) \\ &k = k_s - k_f = k_s - \frac{6}{5L}mg \end{aligned} \tag{17}$$

where x_0, m, k_s, and c are the relative displacement, mass, stiffness and damping constant of the SDOF system, respectively. k_f is the stiffness reduction due to vertical displacement of structural mass and k is the effective stiffness of the structure [32]. Also, F_L represents the hydrodynamic force acting on the tank's wall and can be determined by integrating the liquid pressure distribution along the tank's wall as following:

$$\begin{aligned} F_L = &\int_0^{2\pi}\int_{-h}^{\eta} RP(r,\theta,z,t)\big|_{r=R}\cos\theta\,\mathrm{d}\theta\,\mathrm{d}z = \int_0^{2\pi}\int_{-h}^{0} RP(r,\theta,z,t)\big|_{r=R}\cos\theta\,\mathrm{d}\theta\,\mathrm{d}z \\ &+ \int_0^{2\pi}\int_0^{\eta} RP(r,\theta,z,t)\big|_{r=R}\cos\theta\,\mathrm{d}\theta\,\mathrm{d}z = \int_0^{2\pi}\int_{-h}^{0} RP(r,\theta,z,t)\big|_{r=R}\cos\theta\,\mathrm{d}\theta\,\mathrm{d}z \\ &+ \int_0^{2\pi} R\left[\eta P(R,\theta,0) + \frac{\eta^2}{2}P_z(R,\theta,0) + O(\eta^4)\right]\cos\theta\,\mathrm{d}\theta \end{aligned} \tag{18}$$

where R, h and η are the tank's radius, liquid elevation and the wave amplitude, respectively. Also, $P(r,\theta,z,t)$ is determined from Eq. (15).

3. Boundary conditions

Having assumed a rigid tank, the relative velocity of the fluid along the walls and at the bottom of the tank becomes zero:

$$\left.\frac{\partial\varphi}{\partial r}\right|_{r=R}=0,\quad \left.\frac{\partial\varphi}{\partial z}\right|_{z=-h}=0 \tag{19}$$

Also, the kinetic boundary condition at fluid surface requires the velocity of the fluid surface in the vertical direction be equal to the vertical velocity of the fluid particle at the liquid surface

$$\frac{\partial n}{\partial t}=\frac{\partial\varphi}{\partial z}-\frac{\partial\varphi}{\partial r}\frac{\partial n}{\partial r}-\frac{1}{r^2}\frac{\partial\varphi}{\partial\theta}\frac{\partial n}{\partial\theta} \tag{20}$$

Since, in free surface ($z=\eta$) the pressure is equal to zero, thus

$$\frac{\partial\varphi}{\partial t}+\frac{1}{2}\left\{\left(\frac{\partial\varphi}{\partial r}\right)^2+\frac{1}{r^2}\left(\frac{\partial\varphi}{\partial\theta}\right)^2+\left(\frac{\partial\varphi}{\partial z}\right)^2\right\}+(g-\ddot{\delta})\eta=\ddot{x}_0 r\cos\theta \tag{21}$$

4. Non-dimensional equations

In order to solve Eqs. (15)–(17) with the related boundary conditions given by Eqs. (19)–(21), they were non-dimensionalized using the following parameters:

$$\begin{aligned}
&\bar{x}_0=\frac{x_0}{R},\quad \bar{r}=\frac{r}{R},\quad M=m+m_L,\quad \bar{z}=\frac{z}{R},\quad \bar{\eta}=\frac{\eta}{R},\quad \bar{h}=\frac{h}{R}\\
&\mu_1=\frac{m}{M},\quad \mu_2=\frac{m_L R}{\pi M h},\quad \overline{\varphi}=\frac{\varphi}{R^2\omega_{11}},\quad m_L=\pi\rho R^2 h,\quad \bar{l}=\frac{L}{R},\quad \bar{\delta}=\frac{\delta}{R}\\
&\zeta=\frac{c}{M\omega_{11}},\quad \bar{k}=\frac{k}{M\omega_{11}^2},\quad \bar{p}=\frac{p}{\rho R^2\omega_{11}^2},\quad \tau=\omega_{11}t,\quad t\varepsilon_{mn}=\lambda_{mn}R\\
&\Omega=\frac{\Omega_0}{\omega_{11}},\quad \bar{\ddot{x}}_g=\frac{\ddot{X}_g}{MR\omega_{11}^2},\quad f_L=\frac{F_L}{mR\omega_{11}^2},\quad \overline{\omega}=\frac{\omega_{mn}}{\omega_{11}},\quad \overline{\omega}_{11}=1
\end{aligned} \tag{22}$$

where m_L and M are the liquid mass and total mass of the system, respectively. The parameter ω_{11} is the first asymmetrical liquid frequency given by

$$\omega_{11}^2=\frac{g\varepsilon_{11}}{R}\tanh\left(\varepsilon_{11}\frac{h}{R}\right) \tag{23}$$

Also, Ω_0 is the frequency of the external harmonic excitation and λ_{mn} is the nth positive root of the derivative of the Bessel function, $\mathrm{d}J_m(\lambda_{mn}r)/\mathrm{d}r\big|_{r=R}=0$. The parameters λ_{mn} and ε_{mn} can be computed numerically using any numerical software. The values of ε_{mn} were determined as $\varepsilon_{01}=3.832$, $\varepsilon_{11}=1.841$ and $\varepsilon_{21}=3.05424$. The obtained results are in good agreement with previous analytical and experimental studies [30].

Using Eqs. (22) and (23), the non-dimensional differential equations become

$$\nabla\overline{\varphi}^2=0\Rightarrow\frac{\partial^2\overline{\varphi}}{\partial\bar{r}^2}+\frac{1}{\bar{r}}\frac{\partial\overline{\varphi}}{\partial\bar{r}}+\frac{1}{\bar{r}^2}\frac{\partial^2\overline{\varphi}}{\partial\theta^2}+\frac{\partial^2\overline{\varphi}}{\partial\bar{z}^2}=0 \tag{24}$$

$$\mu_1\ddot{\bar{x}}_0+\zeta\dot{\bar{x}}_0+\bar{k}\bar{x}_0=f_l-\ddot{\bar{x}}_g(t)-\frac{36}{25L^2}\bar{x}_0(\bar{x}_0\ddot{\bar{x}}_0+\dot{\bar{x}}_0^2)$$
$$f_l=\mu_2\int_0^{2\pi}\int_{-\bar{h}}^{0}\bar{p}\cos\theta|_{\bar{r}=1}\,\mathrm{d}\bar{z}\,\mathrm{d}\theta+\mu_2\int_0^{2\pi}\left[\bar{\eta}\bar{p}(1,\theta,0)+\frac{\bar{\eta}^2}{2}\bar{p}_{\bar{z}}(1,\theta,0)\right]\cos\theta\,\mathrm{d}\theta \tag{25}$$

$$\frac{\partial\overline{\varphi}}{\partial\tau}+\frac{1}{2}\left[\left(\frac{\partial\overline{\varphi}}{\partial\bar{r}}\right)^2+\frac{1}{\bar{r}^2}\left(\frac{\partial\overline{\varphi}}{\partial\theta}\right)^2+\left(\frac{\partial\overline{\varphi}}{\partial\bar{z}}\right)^2\right]+\bar{p}+\frac{\bar{z}}{\varepsilon_{11}\tanh(\varepsilon_{11}h)}-\ddot{\bar{\delta}}\bar{z}=-\ddot{\bar{x}}_0\bar{r}\cos\theta \tag{26}$$

with the boundary conditions

$$\left.\frac{\partial\overline{\varphi}}{\partial\bar{r}}\right|_{\bar{r}=1}=0,\quad\left.\frac{\partial\overline{\varphi}}{\partial\bar{z}}\right|_{\bar{z}=\bar{h}}=0 \tag{27}$$

$$\frac{\partial\bar{\eta}}{\partial\tau}=\frac{\partial\overline{\varphi}}{\partial\bar{z}}-\frac{\partial\overline{\varphi}}{\partial\bar{r}}\frac{\partial\bar{\eta}}{\partial\bar{r}}-\frac{1}{\bar{r}^2}\frac{\partial\overline{\varphi}}{\partial\theta}\frac{\partial\bar{\eta}}{\partial\theta}\bigg|_{\bar{z}=\bar{\eta}} \tag{28}$$

$$\bar{z}=\bar{\eta}\rightarrow\bar{p}=0$$
$$\frac{\partial\overline{\varphi}}{\partial\tau}+\frac{1}{2}\left\{\left(\frac{\partial\overline{\varphi}}{\partial\bar{r}}\right)^2+\frac{1}{\bar{r}^2}\left(\frac{\partial\overline{\varphi}}{\partial z}\right)^2+\left(\frac{\partial\overline{\varphi}}{\partial z}\right)^2\right\}+\frac{\bar{\eta}}{\varepsilon_{11}\tanh(\varepsilon_{11}\bar{h})}-\ddot{\bar{\delta}}\bar{\eta}=-\ddot{\bar{x}}_0\bar{r}\cos\theta \tag{29}$$

5. Solution to the governing differential equations

The solution to the Laplace equation given by Eq. (24) with the boundary conditions provided in Eq. (27) is

$$\varphi(r,\theta,z,t)=\sum_{m=1}^{\infty}\sum_{n=1}^{\infty}[a_{mn}(t)\cos m\theta+b_{mn}(t)\sin m\theta]J_{mn}(\varepsilon_{mn}r)\frac{\cos h[\varepsilon_{mn}(z+h)]}{\cos h(\varepsilon_{mn}h)} \tag{30}$$

The non-dimensionalizing symbol "−" for different parameters is removed for simplicity. From the linear part of Eq. (28), η becomes

$$\eta=-\varepsilon_{11}\tanh(\varepsilon_{11}h)\frac{\partial\varphi}{\partial t}(z=0)\Rightarrow\eta=\sum_{m=0}^{\infty}\sum_{n=1}^{\infty}[\alpha_{mn}\cos m\theta+\beta_{mn}\sin m\theta]J_{mn}(\varepsilon_{mn}r) \tag{31}$$

Having assumed a circular cylindrical tank, the parameters β_{mn} and α_{mn} have a phase difference of $\pi/2$. In this study, the excitations as well as the effect of sloshing modes are assumed to be along the x-axis only. Therefore, disregarding the secondary effects of internal resonance between x and y direction sloshing modes, β_{mn} and in a similar way, b_{mn} can be excluded from the equations. Using these assumption and considering the 3 liquid modes of (1,1), (0,1) and (2,1), φ and η can be re-written as

$$\varphi=a_{11}(t)\cos\theta J_1(\varepsilon_{11}r)\frac{\cos h[\varepsilon_{11}(z+h)]}{\cos h(\varepsilon_{11}h)}+a_{01}(t)J_0(\varepsilon_{01}r)\frac{\cos h[\varepsilon_{01}(z+h)]}{\cos h(\varepsilon_{01}h)}$$
$$+a_{21}(t)\cos 2\theta J_2(\varepsilon_{21}r)\frac{\cos h[\varepsilon_{21}(z+h)]}{\cos h(\varepsilon_{21}h)} \tag{32}$$

$$\eta=\alpha_{11}(t)\cos\theta J_1(\varepsilon_{11}r)+\alpha_{01}(t)J_0(\varepsilon_{01}r)+\alpha_{21}(t)\cos 2\theta J_2(\varepsilon_{21}r) \tag{33}$$

in which, α_{mn} and a_{mn} are time-dependent variables that can be determined through satisfying the free surface boundary conditions. Inserting Eqs. (32) and (33) into Eq. (25) for the structure and using the Fourier Dini series (the general form of Fourier series) for r in $\ddot{x}_0 r\cos\theta$ leads to [30]:

$$r=F_nJ_1(\varepsilon_{1n}r) \tag{34}$$

where

$$F_n = \frac{\int_0^R r^2 J_1(\varepsilon_{1n} r)\,\mathrm{d}r}{\int_0^R r J_1^2(\varepsilon_{1n} r)\,\mathrm{d}r} = \frac{2R}{(\varepsilon_{1n}^2 - 1)J_1(\varepsilon_{1n} R)} \tag{35}$$

in Eq. (35), R and F_1 are equal to 1 and 1.4386, respectively. Adapting the same notation used by Ibrahim and Ikeda [24,25], as it is shown in Appendix A, one could obtain:

$$\begin{aligned}
\mu_1\ddot{x}_0 + \zeta\dot{x}_0 + kx_0 = & -\ddot{x}_g(t) - \frac{36}{25L^2}x_0(x_0\ddot{x}_0 + \dot{x}_0^2) - \pi\mu_2\left\{\left(\frac{\varepsilon_{01}\varepsilon_{11}}{\varepsilon_{01}^2 - \varepsilon_{11}^2}\right)\left[(\psi_{01} - \psi_{11})\frac{\mathrm{d}J_1(\varepsilon_{11}r)}{\mathrm{d}r}\frac{\mathrm{d}J_0(\varepsilon_{01}r)}{\mathrm{d}r}\right.\right.\\
& + \left(\frac{\varepsilon_{01}^2\psi_{11} - \varepsilon_{11}^2\psi_{01}}{\varepsilon_{01}\varepsilon_{11}}\right)J_1(\varepsilon_{11})J_0(\varepsilon_{01})\Big]a_{01}a_{11} + \left(\frac{\varepsilon_{11}\varepsilon_{21}}{\varepsilon_{11}^2 - \varepsilon_{21}^2}\right)\left[\frac{1}{2}(\psi_{11} - \psi_{21})\frac{\mathrm{d}J_1(\varepsilon_{11}r)}{\mathrm{d}r}\frac{\mathrm{d}J_2(\varepsilon_{21}r)}{\mathrm{d}r}\right.\\
& + (\psi_{11} - \psi_{21})J_1(\varepsilon_{11})J_2(\varepsilon_{21}) + \frac{1}{2}\left(\frac{\varepsilon_{11}^2\psi_{21} - \varepsilon_{21}^2\psi_{11}}{\varepsilon_{11}\varepsilon_{21}}\right)J_1(\varepsilon_{11})J_2(\varepsilon_{21})\Big]a_{11}a_{21} + \frac{J_1(\varepsilon_{11})\psi_{11}}{\varepsilon_{11}^2}\dot{a}_{11}\\
& + h\ddot{x}_0 + \frac{3}{8}\psi_{11}J_1^3(\varepsilon_{11}r)\alpha_{11}^2\dot{a}_{11} + \frac{3}{8}\left(J_1^3(\varepsilon_{11}r)\left(\frac{1}{3} + \psi_{11}^2\right) + \varepsilon_{11}^2\left(\frac{\mathrm{d}J_1(\varepsilon_{11}r)}{\mathrm{d}r}\right)^2 J_1(\varepsilon_{11})\right)\alpha_{11}a_{11}^2\Big\}_{r=1}
\end{aligned} \tag{36}$$

Expanding Eqs. (28) and (29) at $\eta = 0$ and using the same approach results in

$$\begin{aligned}
& \left[\dot{a}_{11} + \frac{\alpha_{11}}{\psi_{11}} + \frac{2\ddot{x}_0}{(\varepsilon_{11}^2 - 1)J_1(\varepsilon_{11})} + \frac{2}{(\varepsilon_{11}^2 - 1)J_1(\varepsilon_{11})}\left[\ddot{x}_g(t) + \frac{36}{25l^2}x_0(\dot{x}_0^2 + x_0\ddot{x}_0)\right] - \frac{6}{5l}(\dot{x}_0^2 + x_0\ddot{x}_0)\alpha_{11}\right.\\
& + \gamma_1^{110}\varepsilon_{01}\varepsilon_{11}a_{11}a_{01} + \frac{1}{2}\gamma_1^{112}\varepsilon_{11}\varepsilon_{21}a_{11}a_{21} + U_1^{021}a_{11}a_{21} + K_1^{120}\psi_{01}\psi_{11}a_{11}a_{01}\\
& + \frac{1}{2}K_1^{021}\psi_{11}\psi_{21}a_{11}a_{21} + \psi_{01}K_1^{120}\dot{a}_{01}\alpha_{11} + \psi_{11}K_1^{120}\dot{a}_{11}\alpha_{01} + \frac{1}{2}\psi_{11}K_1^{021}\dot{a}_{11}\alpha_{21}\\
& + \frac{1}{2}\psi_{21}K_1^{021}\dot{a}_{21}\alpha_{11} + \frac{3}{4}\varepsilon_{11}^2\psi_{11}\Gamma_1^{1111}a_{11}^2\alpha_{11} + \frac{1}{4}u_1^{040}\psi_{11}a_{11}^2\alpha_{11} + \frac{3}{4}\varepsilon_{11}^2\psi_{11}K_1^{040}a_{11}^2\alpha_{11}\\
& \left.+ \frac{3}{8}\varepsilon_{11}^2K_1^{040}\dot{a}_{11}\alpha_{11}^2\right]\cos\theta J_1(\varepsilon_{11}r) + \left[\dot{a}_{01} + \frac{\alpha_{01}}{\psi_{11}} - \frac{6}{5l}(\dot{x}_0^2 + x_0\ddot{x}_0)\alpha_{01} + \frac{1}{4}\varepsilon_{11}^2\gamma_0^{011}a_{11}^2 + \frac{1}{4}U_0^{120}a_{11}^2\right.\\
& \left.+ \frac{1}{4}\psi_{11}^2K_0^{120}a_{11}^2 + \frac{1}{2}\psi_{11}K_0^{120}\dot{a}_{11}\alpha_{11}\right]J_0(\varepsilon_{01}r) + \left[\dot{a}_{21} + \frac{\alpha_{21}}{\psi_{11}} - \frac{6}{5l}(\dot{x}_0^2 + x_0\ddot{x}_0)\alpha_{21} + \frac{1}{4}\varepsilon_{11}^2\gamma_2^{211}a_{11}^2\right.\\
& \left.- \frac{1}{4}U_2^{021}a_{11}^2 + \frac{1}{4}K_2^{021}\psi_{11}^2a_{11}^2 + \frac{1}{2}\psi_{11}K_2^{021}\dot{a}_{11}\alpha_{11}\right]\cos 2\theta J_2(\varepsilon_{21}r) = 0
\end{aligned} \tag{37}$$

$$\begin{aligned}
& \left[\dot{\alpha}_{11} - \psi_{11}K_1^{020}a_{11} + \gamma_1^{110}\varepsilon_{01}\varepsilon_{11}(a_{11}\alpha_{01} + a_{01}\alpha_{11}) + \frac{1}{2}\gamma_1^{112}\varepsilon_{11}\varepsilon_{21}(a_{21}\alpha_{11} + a_{11}\alpha_{21})\right.\\
& - \varepsilon_{01}^2K_1^{120}a_{01}\alpha_{11} - \varepsilon_{11}^2K_1^{120}a_{11}\alpha_{01} - \frac{1}{2}\varepsilon_{11}^2K_1^{021}a_{11}\alpha_{21} - \frac{1}{2}\varepsilon_{21}^2K_1^{021}a_{21}\alpha_{11}\\
& \left.+ U_1^{021}(a_{21}\alpha_{11} + a_{11}\alpha_{21}) + \frac{3}{4}\varepsilon_{11}^2\psi_{11}\Gamma_1^{1111}a_{11}\alpha_{11}^2 + \frac{1}{4}U_1^{040}\psi_{11}a_{11}\alpha_{11}^2 - \frac{3}{8}K_1^{040}\psi_{11}\varepsilon_{11}^2a_{11}\alpha_{11}^2\right]\cos\theta J_1(\varepsilon_{11}r)\\
& + \left[\dot{\alpha}_{01} - \psi_{01}K_0^{200}a_{01} + \frac{1}{2}\varepsilon_{11}^2\gamma_0^{011}a_{11}\alpha_{11} - \frac{1}{2}\varepsilon_{11}^2K_0^{120}a_{11}\alpha_{11} + \frac{1}{2}U_0^{120}a_{11}\alpha_{11}\right]J_0(\varepsilon_{01}r)\\
& + \left[\dot{\alpha}_{21} - \psi_{21}K_2^{002}a_{21} + \frac{1}{2}\varepsilon_{11}^2\gamma_2^{211}\varepsilon_{11}^2a_{11}\alpha_{11} - \frac{1}{2}\varepsilon_{11}^2K_2^{021}a_{11}\alpha_{11} - \frac{1}{2}U_2^{021}a_{11}\alpha_{11}\right]\cos 2\theta J_2(\varepsilon_{21}r) = 0
\end{aligned} \tag{38}$$

Equating the coefficients of $J_0(\varepsilon_{01}r)$, $J_1(\varepsilon_{11}r)\cos\theta$ and $J_2(\varepsilon_{21}r)\cos 2\theta$ to zero and using the following assumptions:

$$\begin{aligned}&\alpha_{11}, a_{11}, x = O(\eta)\\ &\alpha_{01}, \alpha_{21}, a_{01}, a_{21} = O(\eta^2)\\ &\alpha_{mn}, a_{mn} = O(\eta^m)\end{aligned} \tag{39}$$

Would lead to the following non-dimensional governing differential equations of the system if one eliminates all the terms higher than $O(\eta^3)$:

$$(\mu_1+\mu_2\pi h)\ddot{x}_0+\frac{36}{25l^2}x_0(\dot{x}_0^2+x_0\ddot{x}_0)+\zeta\dot{x}_0+kx_0+G_2\dot{a}_{11}+G_3a_{01}a_{11}+G_4a_{11}a_{21}+G_5\alpha_{11}^2\dot{a}_{11}+G_6\alpha_{11}a_{11}^2=-\ddot{x}_g(t) \tag{40}$$

$$\begin{aligned}&\dot{a}_{11}+G_1\ddot{x}_0+G_1\left[\ddot{x}_g(t)+\frac{36}{25l^2}x_0(\dot{x}_0^2+x_0\ddot{x}_0)\right]-\frac{6}{5l}(\dot{x}_0^2+x_0\ddot{x}_0)\alpha_{11}+\frac{1}{\psi_{11}}\alpha_{11}+Q_4\dot{a}_{01}\alpha_{11}\\ &+Q_5\dot{a}_{11}\alpha_{01}+Q_6\dot{a}_{11}\alpha_{21}+Q_7\dot{a}_{21}\alpha_{11}+Q_8\dot{a}_{11}\alpha_{11}^2+Q_9a_{01}\alpha_{11}+Q_{10}a_{11}\alpha_{21}+Q_{11}a_{11}^2\alpha_{11}=0\end{aligned} \tag{41}$$

$$\dot{a}_{01}+\frac{1}{\psi_{01}}\alpha_{01}+Q_{12}\dot{a}_{11}\alpha_{11}+Q_{13}a_{11}^2-\frac{6}{5l}(\dot{x}_0^2+x_0\ddot{x}_0)\alpha_{01}=0 \tag{42}$$

$$\dot{a}_{21}+\frac{1}{\psi_{21}}\alpha_{21}+Q_{14}\dot{a}_{11}\alpha_{11}+Q_{15}a_{11}^2-\frac{6}{5l}(\dot{x}_0^2+x_0\ddot{x}_0)\alpha_{21}=0 \tag{43}$$

$$\dot{\alpha}_{11}-\psi_{11}a_{11}+Q_{16}a_{01}\alpha_{11}+Q_{17}a_{11}\alpha_{01}+Q_{18}a_{11}\alpha_{21}+Q_{19}a_{21}\alpha_{11}+Q_{20}a_{11}\alpha_{11}^2=0 \tag{44}$$

$$\dot{\alpha}_{01}-\psi_{01}a_{01}+Q_{21}a_{11}\alpha_{11}=0 \tag{45}$$

$$\dot{\alpha}_{21}-\psi_{21}a_{21}+Q_{22}a_{11}\alpha_{11}=0 \tag{46}$$

All the above coefficients are defined in Appendix B.

Eliminating the parameters a_{11}, a_{01}, a_{21} from Eqs. (40)–(46) and retaining the terms up to $O(\eta^3)$, would result in the following governing differential equations for the system:

$$\begin{aligned}&\ddot{\alpha}_{01}+\omega_{01}^2\alpha_{01}+2\zeta_0\omega_{01}\dot{\alpha}_{01}(t)-\frac{6}{5l}(\dot{x}_0^2+x_0\ddot{x}_0)\psi_{01}\alpha_{01}+\left(\frac{Q_{21}+\psi_{01}Q_{12}}{\psi_{11}}\right)\alpha_{11}\ddot{\alpha}_{11}\\ &+\left(\frac{Q_{21}}{\psi_{11}}+\frac{Q_{13}\psi_{01}}{\psi_{11}^2}\right)\dot{\alpha}_{11}^2+(Q_{21}+Q_{12}\psi_{01})S_6\ddot{\alpha}_{11}\alpha_{11}^2+(Q_{21}+Q_{12}\psi_{01})S_2\alpha_{11}\ddot{\alpha}_{01}\\ &+(Q_{21}+Q_{12}\psi_{01})S_3\alpha_{11}\ddot{\alpha}_{21}+\left[(Q_{21}+Q_{12}\psi_{01})S_6+S_6Q_{21}+\frac{2S_6Q_{13}\psi_{01}}{\psi_{11}}\right]\alpha_{11}\dot{\alpha}_{11}^2\\ &+\left(Q_{21}S_2+\frac{2S_2Q_{13}\psi_{01}}{\psi_{11}}\right)\dot{\alpha}_{11}\dot{\alpha}_{01}+\left(Q_{21}S_3+\frac{2S_3Q_{13}\psi_{01}}{\psi_{11}}\right)\dot{\alpha}_{11}\dot{\alpha}_{21}=0\end{aligned} \tag{47}$$

$$\begin{aligned}&\ddot{\alpha}_{21}+\omega_{21}^2\alpha_{21}+2\zeta_2\omega_{21}\dot{\alpha}_{21}(t)-\frac{6}{5l}(\dot{x}_0^2+x_0\ddot{x}_0)\psi_{21}\alpha_{21}+\left(\frac{Q_{22}+\psi_{21}Q_{14}}{\psi_{11}}\right)\alpha_{11}\ddot{\alpha}_{11}\\ &+\left(\frac{Q_{22}}{\psi_{11}}+\frac{Q_{15}\psi_{21}}{\psi_{11}^2}\right)\dot{\alpha}_{11}^2+(Q_{22}+Q_{14}\psi_{21})S_6\ddot{\alpha}_{11}\alpha_{11}^2+(Q_{22}+Q_{14}\psi_{21})S_2\alpha_{11}\ddot{\alpha}_{01}\\ &+(Q_{22}+Q_{14}\psi_{21})S_3\alpha_{11}\ddot{\alpha}_{21}+\left[(Q_{22}+\psi_{21}Q_{14})S_6+Q_{22}S_6+\frac{2S_6Q_{15}\psi_{21}}{\psi_{11}}\right]\alpha_{11}\dot{\alpha}_{11}^2\\ &+\left(Q_{22}S_2+\frac{2S_2\psi_{21}Q_{15}}{\psi_{11}}\right)\dot{\alpha}_{11}\dot{\alpha}_{01}+\left(Q_{22}S_3+\frac{2S_3Q_{15}\psi_{21}}{\psi_{11}}\right)\dot{\alpha}_{21}\dot{\alpha}_{11}=0\end{aligned} \tag{48}$$

$$G_0\ddot{x}_0+\frac{36}{25l^2}x_0(\dot{x}_0^2+x_0\ddot{x}_0)+kx_0+\frac{G_2}{\psi_{11}}\ddot{\alpha}_{11}+\zeta\dot{x}_0+G_2S_2\ddot{\alpha}_{01}+G_2S_3\ddot{\alpha}_{21}+G_2S_6\ddot{\alpha}_{11}\alpha_{11}$$
$$+G_2S_6\dot{\alpha}_{11}^2+\left(\frac{G_3}{\psi_{01}\psi_{11}}+(S_4+S_7)G_2\right)\dot{\alpha}_{01}\dot{\alpha}_{11}+\left(\frac{G_4}{\psi_{21}\psi_{11}}+(S_5+S_8)G_2\right)\dot{\alpha}_{21}\dot{\alpha}_{11}$$
$$+\left(\frac{G_3Q_{21}}{\psi_{01}\psi_{11}^2}+\frac{G_4Q_{22}}{\psi_{21}\psi_{11}^2}+2S_9G_2\right)\alpha_{11}\dot{\alpha}_{11}^2+G_2S_4\ddot{\alpha}_{01}\alpha_{11}+G_2S_5\ddot{\alpha}_{21}\alpha_{11}$$
$$+G_2S_7\ddot{\alpha}_{11}\alpha_{01}+G_2S_8\ddot{\alpha}_{11}\alpha_{21}+G_2S_9\ddot{\alpha}_{11}\alpha_{11}^2+G_5\frac{\alpha_{11}^2\ddot{\alpha}_{11}}{\psi_{11}}+G_6\frac{\alpha_{11}\ddot{\alpha}_{11}^2}{\psi_{11}^2}=-\ddot{x}_g(t) \tag{49}$$

$$\ddot{\alpha}_{11}+\omega_{11}^2\alpha_{11}+G_1\psi_{11}\ddot{x}_0+2\zeta_1\dot{\alpha}_{11}(t)+G_1\psi_{11}\left[\ddot{x}_g(t)+\frac{36}{25l^2}x_0(\dot{x}_0^2+x_0\ddot{x}_0)\right]-\frac{6}{5l}(\dot{x}_0^2+x_0\ddot{x}_0)\alpha_{11}$$
$$+\psi_{11}S_6\dot{\alpha}_{11}^2+\psi_{11}S_2\ddot{\alpha}_{01}+\psi_{11}S_3\ddot{\alpha}_{21}+\psi_{11}S_6\ddot{\alpha}_{11}\alpha_{11}+\left(\frac{Q_4}{\psi_{01}}+S_4\right)\psi_{11}\alpha_{11}\ddot{\alpha}_{01}$$
$$+\left(\frac{Q_{21}Q_4}{\psi_{01}}+\frac{Q_{22}Q_7}{\psi_{21}}+Q_8+\psi_{11}S_9\right)\ddot{\alpha}_{11}\alpha_{11}^2+(Q_5+S_7\psi_{11})\ddot{\alpha}_{11}\alpha_{01}+(Q_6+S_8\psi_{11})\ddot{\alpha}_{11}\alpha_{21}$$
$$+\left(\frac{Q_{21}Q_4}{\psi_{01}}+\frac{Q_{22}Q_7}{\psi_{21}}+\frac{Q_{22}Q_{10}}{\psi_{21}\psi_{11}}+\frac{Q_{11}}{\psi_{11}}+\frac{Q_9Q_{21}}{\psi_{01}\psi_{11}}+2S_9\psi_{11}\right)\alpha_{11}\dot{\alpha}_{11}^2+\left(\frac{Q_7}{\psi_{21}}+S_5\right)\psi_{11}\ddot{\alpha}_{21}\alpha_{11}$$
$$+\left(\frac{Q_9}{\psi_{01}}+\psi_{11}(S_4+S_7)\right)\dot{\alpha}_{01}\dot{\alpha}_{11}+\left(\frac{Q_{10}}{\psi_{21}}+\psi_{11}(S_5+S_8)\right)\dot{\alpha}_{21}\dot{\alpha}_{11}=0 \tag{50}$$

In order to consider the energy dissipation capacity of the sloshing modes, also viscous damping terms were introduced to the modal equations of the liquid sloshing modes. The parameters S_2–S_9 are described in Appendix C. Finally, Eqs. (47)–(50) can be numerically solved to determine the response of the SDOF structural system and the amplitude of liquid sloshing modes.

Omitting the parameters related to the (0,1) and (2,1) sloshing modes as well as the effect of wave amplitude η on lateral dynamic pressure from Eqs. (49) and (50), would result in two simplified equations for the system with 1 sloshing mode under lateral excitation. These simplified equations are in total agreement with those provided by Ibrahim et al. in their previous work [10].

6. Numerical example

The derived differential equations of motion are numerically solved for harmonic and earthquake excitation input at resonance cases 1:1 and 1:2. A parametric study is carried out using two liquid mass and two h/R ratios, i.e., $m_L=0.02$, 0.1 M, $h/R=1$ and 0.5. The response of the elastic structure containing the liquid tank for the cases with 3 and 1 sloshing modes is compared with those of the SDOF system alone. Consideration of higher sloshing modes does not have any significant effect on the response of the system [30]. Therefore, the results of 3-mode model will be used as a basis to determine the accuracy of the other approximate models. The damping ratio of the SDOF system is considered to be 2%. Also, the modal damping ratio of the liquid sloshing modes, ε_0, ε_1, and ε_2 are assumed to be 1%. Furthermore, the initial values used for different parameters in this study are: $(\alpha_{01})_0=(\alpha_{21})_0=x_0=0.001$ and $(\alpha_{11})_0=0.005$. The amplitude of the non-dimensional external excitation is assumed to be 0.001 ($\bar{\ddot{x}}_g=0.001\cos\Omega t$). The MATLAB 7.0 software is used to perform the numerical computation.

6.1. Harmonic excitation (resonance case 1:1)

In this case, the external harmonic excitation frequency, Ω, is assumed to be equal to both the system's natural frequency and the frequency of the first unsymmetrical liquid's sloshing mode ($\omega_{11}=\omega_s=\Omega$). Figs. 3(a) and (c), present the lateral response of the structure (x) and the wave height η at the tank's wall for the case of $h/R=0.5$ and $m_l=0.1$ M. Also, the response Fourier transforms and the liquid profile at the time

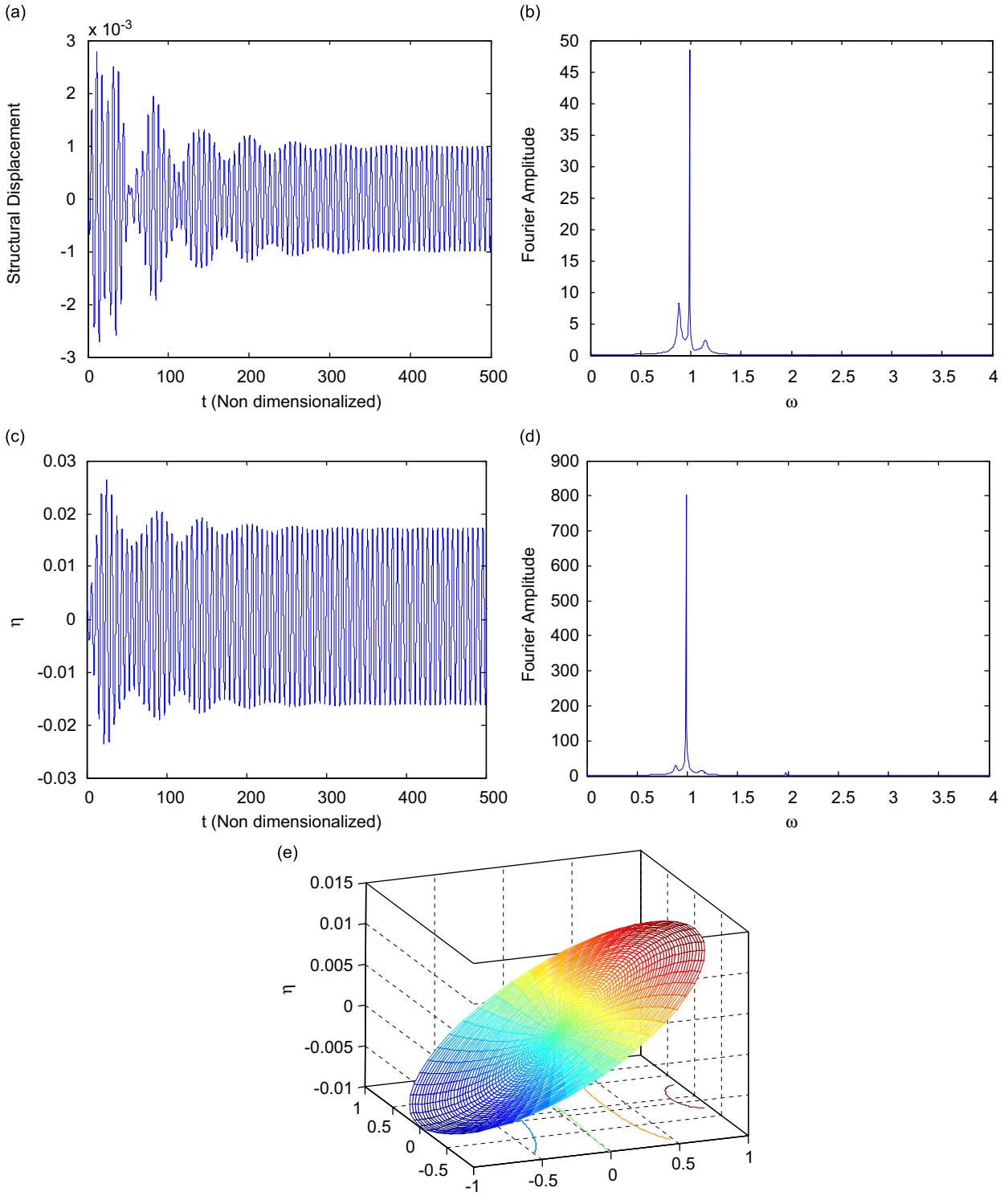

Fig. 3. Structure with liquid tank, 3 sloshing modes case for harmonic excitation at 1:1 resonance, $h/R = 0.5$, $m_L = 0.1\,\mathrm{M}$: (a) structural displacement, (b) Fourier amplitude of structural displacement, (c) wave amplitude η, (d) Fourier amplitude of η, and (e) liquid profile at maximum wave height.

of maximum wave height are shown in Figs. 3(b), (d) and (e). As Fig. 3(a) shows, unlike the SDOF system alone, the structural response in system with liquid tank decays rapidly after achieving its peak. Fig. 4 illustrates the modal amplitude of the first 3 liquid sloshing modes and their Fourier amplitudes. Comparing Figs. 3(c), (e) and 4, proves that the maximum wave height and the related liquid profile is dominated by the effect of the first unsymmetrical sloshing mode for this mass ratio. Maximum response of the liquid modes and the structural system are presented in Table 1 for four different cases. The results indicate that increasing the mass ratio and decreasing h/R ratio improves the performance of the liquid tank in reducing the response of the structural system. For the mass ratio $m_L = 0.1\,\mathrm{M}$, the response of the structural system is reduced significantly with a maximum around 10% of the peak response of the SDOF system alone. There is less reduction in response of the system for the mass ratio $m_L = 0.02\,\mathrm{M}$ with its maximum displacement being around 40% of SDOF system's peak response. The energy transfer from the SDOF system to the liquid and

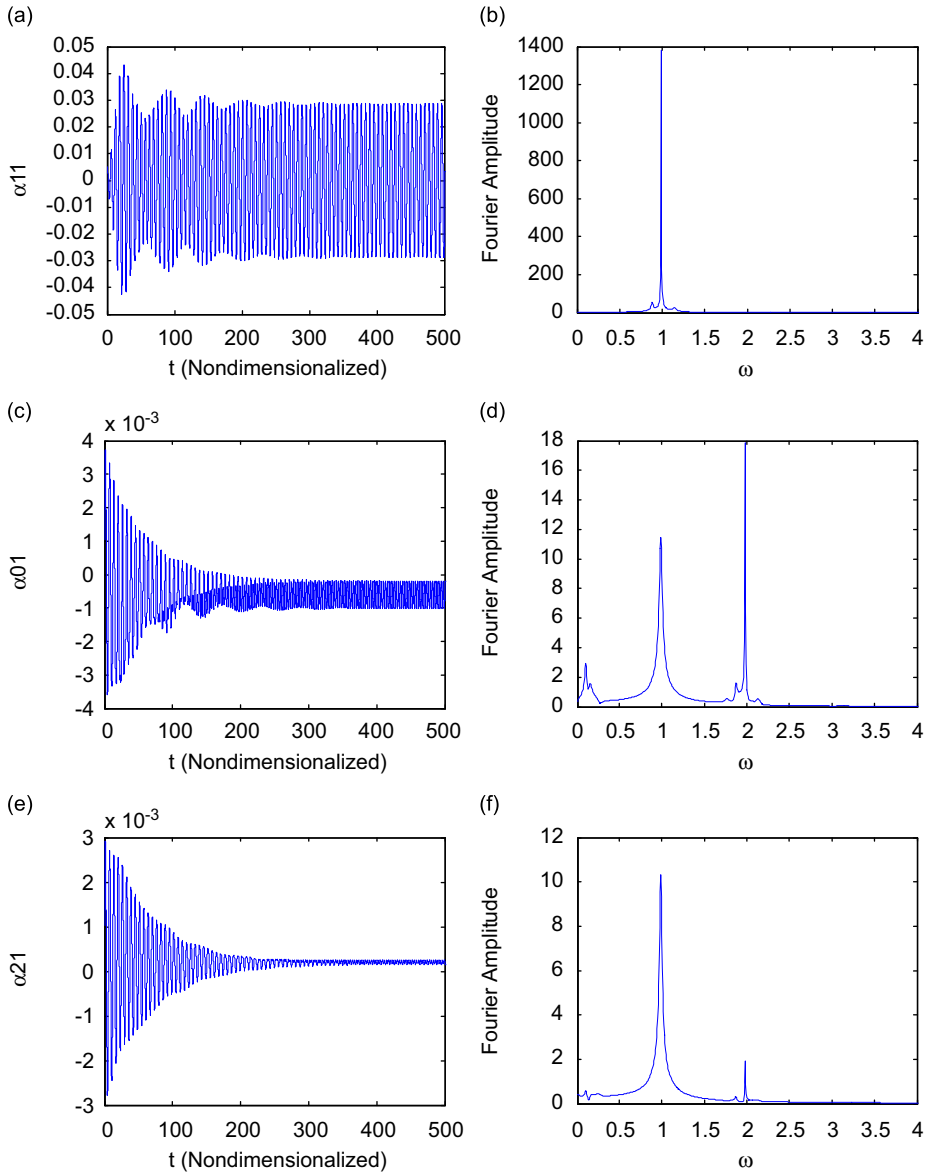

Fig. 4. Liquid modal amplitude for harmonic excitation at 1:1 resonance, $h/R = 0.5$, $m_L = 0.1\,\mathrm{M}$: (a) α_{11}, liquid first asymmetric modal amplitude, (b) Fourier amplitude of α_{11}, (c) α_{01}, liquid (0,1) modal amplitude, (d) Fourier amplitude of α_{01}, (e) α_{21}, liquid (2,1) modal amplitude, and (f) Fourier amplitude of α_{21}.

Table 1
Harmonic excitation—resonance case 1:1 ($\omega_{11} = \omega_s = \Omega$)

Structural model		Maximum response[a]					Reduction (%)[b]	Approximation (%)[c]		
		x	η	α_{11}	α_{01}	α_{21}		x	η	α_{11}
$h/R = 1$	Structure with tank considering 3 sloshing modes	0.0038	0.0540	0.0873	0.0067	0.0045	84.8	–	–	–
$m_L = 0.1\,\mathrm{M}$	Structure with tank considering 1 sloshing mode	0.0038	0.0510	0.0877	–	–	84.8	0.0	5.5	0.4
$h/R = 0.5$	Structure with tank considering 3 sloshing modes	0.0028	0.0264	0.0432	0.0037	0.0029	88.8	–	–	–
$m_L = 0.1\,\mathrm{M}$	Structure with tank considering 1 sloshing mode	0.0028	0.0252	0.0433	–	–	88.8	0.0	4.5	0.2
$h/R = 1$	Structure with tank considering 3 sloshing modes	0.0103	0.1788	0.2498	0.0667	0.0229	58.8	–	–	–
$m_L = 0.02\,\mathrm{M}$	Structure with tank considering 1 sloshing mode	0.0081	0.2039	0.3495	–	–	67.6	21.4	14.0	40.0
$h/R = 0.5$	Structure with tank considering 3 sloshing modes	0.0085	0.1150	0.1623	0.1010	0.1128	66.0	–	–	–
$m_L = 0.02\,\mathrm{M}$	Structure with tank considering 1 sloshing mode	0.0070	0.1130	0.1940	–	–	72.0	17.6	1.7	19.5
SDOF system		0.0250	–	–	–	–	–	–	–	–

[a]Results are provided for the nondimensionalized parameters.
[b]The reduction in the peak response of the structural model is determined with respect to the SDOF system.
[c]Approximation is determined with respect to the 3 modes sloshing model as the most accurate case.

the shift in modal frequencies of the system with tank are considered as the dominant factors in reducing the lateral response of the structure.

The displacement of the SDOF system, and the system containing liquid tank are compared in Fig. 5, for the case of $h/R = 0.5$ and $m_l = 0.02\,\mathrm{M}$ considering 1 and 3 sloshing modes. The results indicate that the liquid tanks with this type of resonance can significantly reduce the response of system including its peak values.

In Fig. 6, the time history of the wave height η at the tank's wall are compared for the 1 and 3 sloshing mode cases, assuming $h/R = 0.5$ and $m_l = 0.02\,\mathrm{M}$. As expected, the results provided in these figures and Table 1, indicate that considering only 1 sloshing mode, in spite of its acceptable performance in certain cases, is not generally adequate for capturing the true behavior of the system. The difference between the results of the 1 and 3 mode models can be up to 14% in determining the maximum wave height η and up to 21% in calculating the maximum structural displacement. That clearly shows the importance of the (0,1) and (2,1) sloshing modes on the maximum wave height and/or peak structural response as it is shown in Figs. 5 and 6 for the 1:1 resonance case.

6.2. Harmonic excitation (resonance case 1:2)

Retaining the linear parts of Eqs. (49) and (50), and neglecting the nonlinear terms, the considered dynamic system reduces to a simplified two degrees of freedom model. The vibrational frequencies of the new simplified system include B_3, which is mainly a structural mode, and B_4, that is dominated by the (1,1) sloshing mode of the liquid. These frequencies can be determined from the following equations:

$$B_3 = \frac{\sqrt{-B_1 - \sqrt{B_1^2 - 4B_2}}}{\sqrt{2}}, \quad B_4 = \frac{\sqrt{-B_1 + \sqrt{B_1^2 - 4B_2}}}{\sqrt{2}} \tag{51}$$

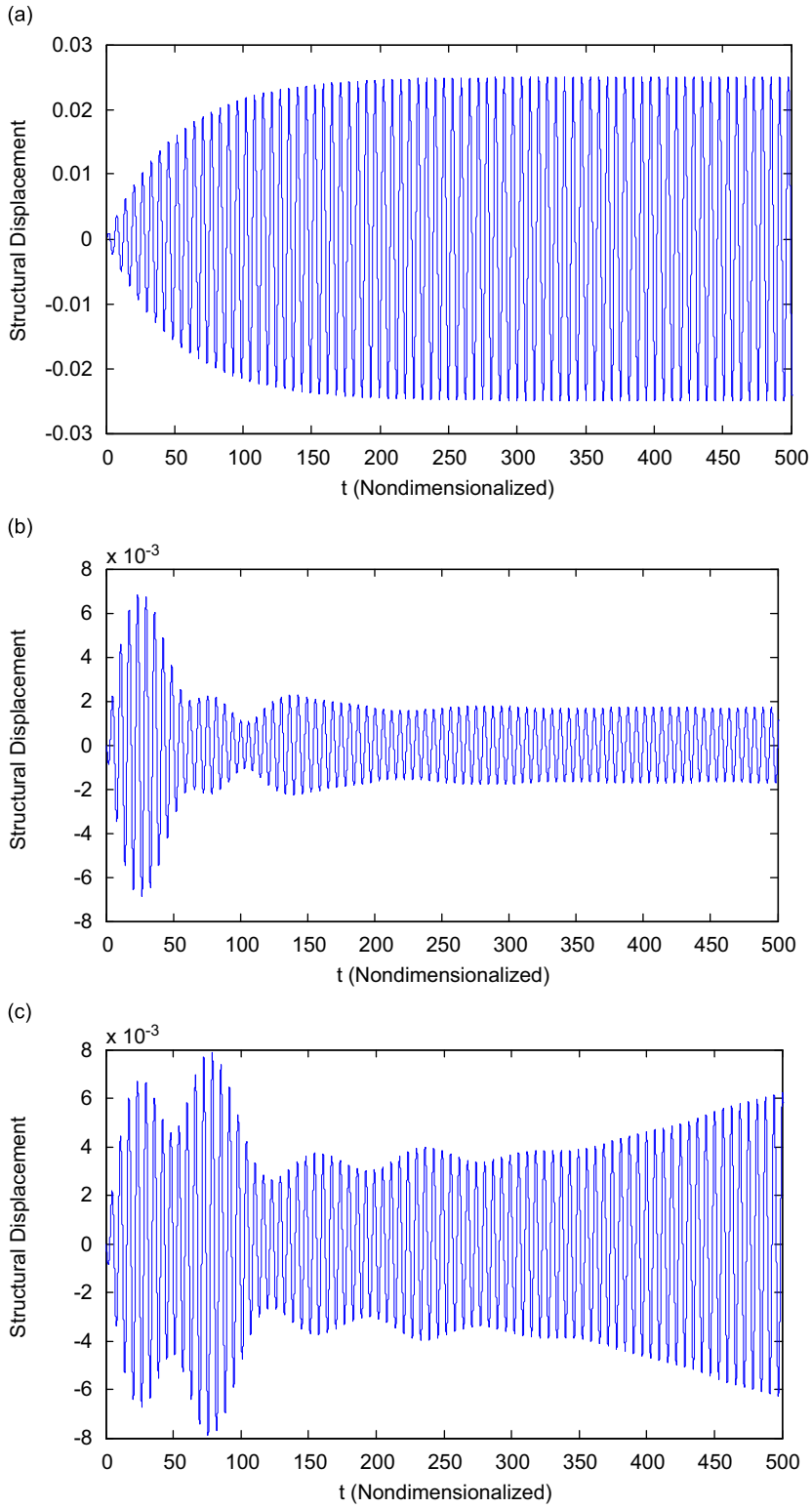

Fig. 5. Structural displacement for harmonic excitation at 1:1 resonance, $h/R = 0.5$, $m_L = 0.02\,\mathrm{M}$: (a) SDOF system, (b) structure with liquid tank—1 sloshing mode, and (c) structure with liquid tank—3 sloshing modes.

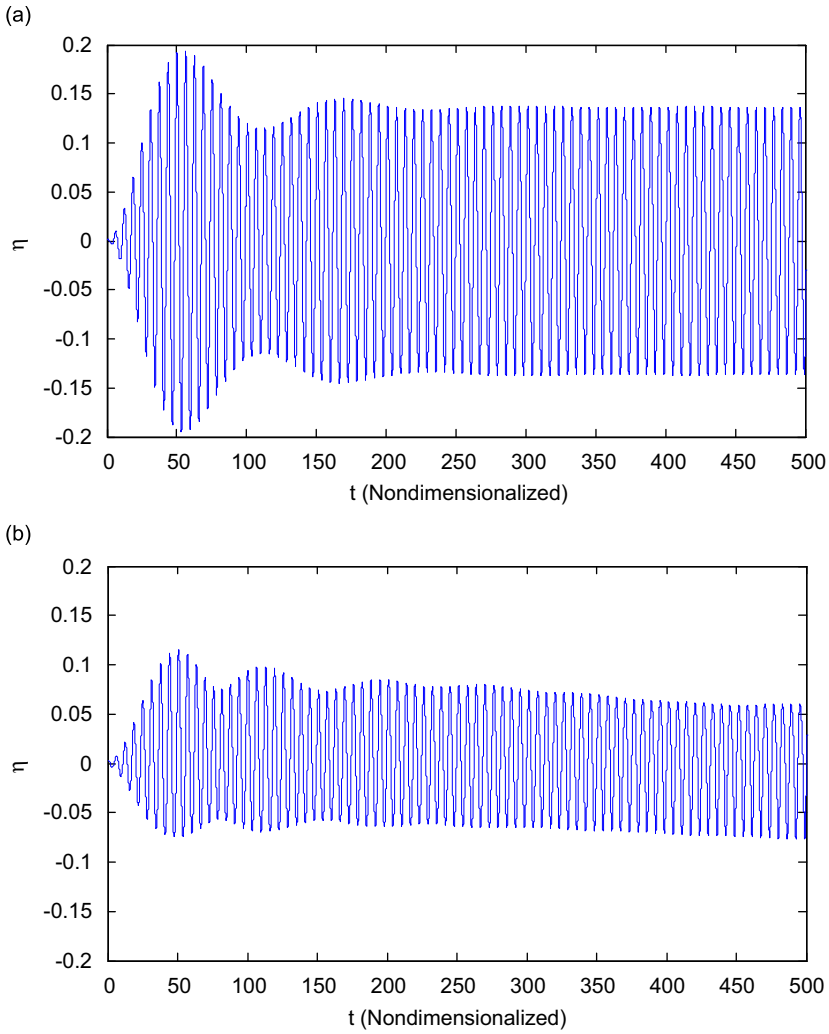

Fig. 6. Wave amplitude η for harmonic excitation at 1:1 resonance, $h/R = 0.5$, $m_L = 0.02$ M: (a) structure with liquid tank—1 sloshing mode and (b) structure with liquid tank—3 sloshing modes.

where B_1 and B_2 are defined as

$$B_1 = \frac{k + G_0}{G_0 - G_1 G_2}, \quad B_2 = \frac{k}{G_0 - G_1 G_2} \tag{52}$$

The parameters G_0, G_1 and G_2 are given in Appendix B. In the (1:2) resonance case, the external harmonic excitation frequency, Ω, and the system's natural frequency ω_s, are determined such that the frequencies of the combined system (B_3 and B_4) to be in the form of $B_3 = 2B_4 = \Omega$.

Inserting for G_0, G_1 and G_2 in the above equations from Appendix B, $G_0 - G_1 G_2$ and consequently the B_1 and B_2 parameters become less than zero if $\left(m_l D/1.3Mh\right)\tanh(1.8h/R) > 1$. Therefore, the modal eigenvalues of the system will have a positive real part. It means that if those modes be excited directly or indirectly through nonlinear interaction, the system response will increase with time and becomes unbounded. For example for the case of $h/r = 0.5$, if $m_L > 0.81$ M, then the system becomes unstable under external excitation frequencies near to the modal frequencies of the system. For small h/r ratios (less than 0.1), traveling waves will be generated. Also, under the severe external excitations, the wave amplitude η may become larger than 0.75 h,

Table 2
Harmonic excitation—resonance case 1:2 ($2B_4 = B_3 = \Omega$)

Structural model		Model parameters[a]					Reduction (%)[b]	Approximation (%)[c]		
		x	η	α_{11}	α_{01}	α_{21}		x	η	α_{11}
$h/R = 1$	Structure with tank considering 3 sloshing modes	0.0061	0.1086	0.1150	0.0594	0.0621	12.9	–	–	–
$m_L = 0.1\,\mathrm{M}$	Structure with tank considering 1 sloshing mode	0.0061	0.1250	0.2150	–	–	12.9	0	15.1	87
$h/R = 0.5$	Structure with tank considering 3 sloshing modes	0.0060	0.0633	0.0749	0.0427	0.0235	14.3	–	–	–
$m_L = 0.1\,\mathrm{M}$	Structure with tank considering 1 sloshing mode	0.0060	0.0966	0.1660	–	–	14.3	0	52.6	99.8
$h/R = 1$	Structure with tank considering 3 sloshing modes	0.0062	0.2025	0.2309	0.1023	0.1294	11.4	–	–	–
$m_L = 0.02\,\mathrm{M}$	Structure with tank considering 1 sloshing mode	0.0062	0.1280	0.2200	–	–	11.4	0	36.8	4.7
$h/R = 0.5$	Structure with tank considering 3 sloshing modes	0.0062	0.1173	0.1417	0.0784	0.0578	11.4	–	–	–
$m_L = 0.02\mathrm{M}$	Structure with tank considering 1 sloshing mode	0.0062	0.1251	0.2150	–	–	11.4	0	11.7	83
SDOF system			–	–	–	–	–	–	–	–

[a]Results are provided for the nondimensionalized parameters.
[b]The reduction in the peak response of the structural model is determined with respect to the SDOF system.
[c]Approximation is determined with respect to the 3 modes sloshing model as the most accurate case.

leading to wave breaking phenomenon. In that case, the derived governing differential equations of motion lose their credibility to be used in this study.

Maximum responses of the liquid sloshing modes and the structural system are presented in Table 2 for different h/R and m_L ratios at the 1:2 resonance case. Fig. 7 shows the response of the structure and the wave height η at the tank walls and their Fourier amplitudes for the case of $h/R = 0.5$ and $m_L = 0.1\,\mathrm{M}$. As it is shown, the structural response decreases appreciably in time (time is non-dimensionalized) after going through its peak value, meaning an increase in energy transfer to liquid with time. Fig. 7(b) shows the Fourier amplitude of the structural responses that have two major peaks at system's natural frequency and liquid's first asymmetric modal frequency. This means that even if the liquid is not excited directly, due to nonlinear interaction between the liquid and the structure, energy transfer from the structure to liquid is taking place causing an increase in liquid response with time. Therefore, the response of the structure as Fig. 7(a) illustrates, would be decreasing.

Fig. 7(e) shows the liquid profile as the wave amplitude η achieves its maximum value. As this figure shows, the liquid profile for the case with 3 sloshing modes is completely different from its asymmetric shape for the case with 1 sloshing mode. That clearly indicates the importance of considering more number of sloshing modes in determining the liquid's profile. However, the location of the maximum wave height (η) still remains at the boundaries of the tank.

The modal amplitude of 3 liquid sloshing modes and their Fourier amplitudes for the above case are shown in Fig. 8. As this figure presents, the effect of (0,1) and (2,1) sloshing modes on the amplitude of liquid wave η are considerably increased. This effect for models with $m_L = 0.1\,\mathrm{M}$ and smaller h/R ratios are more considerable.

Figs. 9 and 10 compare the lateral response of the SDOF system and the system equipped with liquid tank, as well as the wave height η at the tank's boundary, for the 1 and 3 sloshing modes cases. These figures show that the case with 1 sloshing mode can appropriately estimate the peak response of the system, but it does not provide a good estimate of the decay in system response with time.

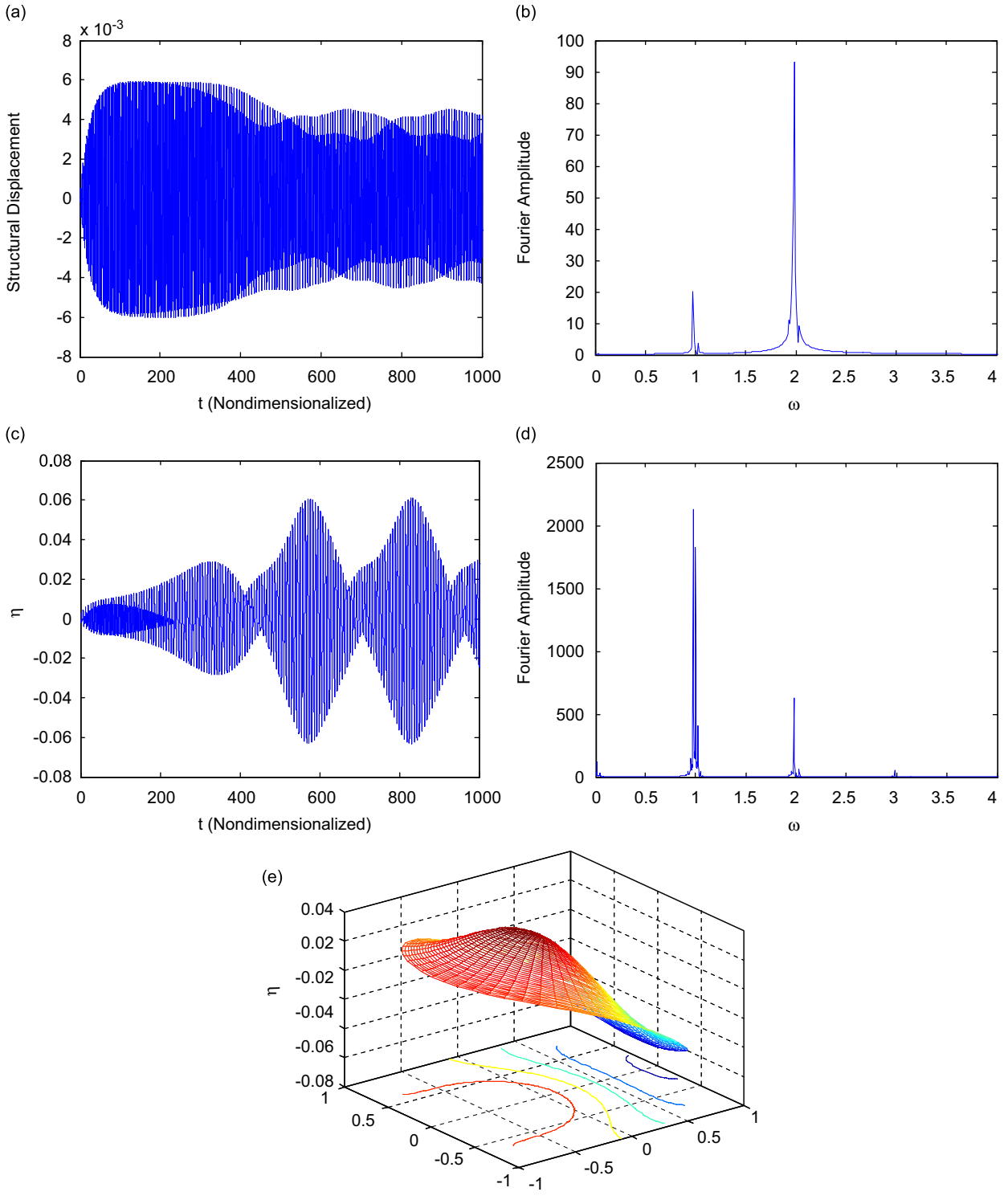

Fig. 7. Structure with liquid tank, 3 sloshing modes case for harmonic excitation at 1:2 resonance, $h/R = 0.5$, $m_L = 0.1$ M: (a) structural displacement, (b) Fourier amplitude of structural displacement, (c) wave amplitude η, (d) Fourier amplitude of η, and (e) liquid profile at maximum wave height.

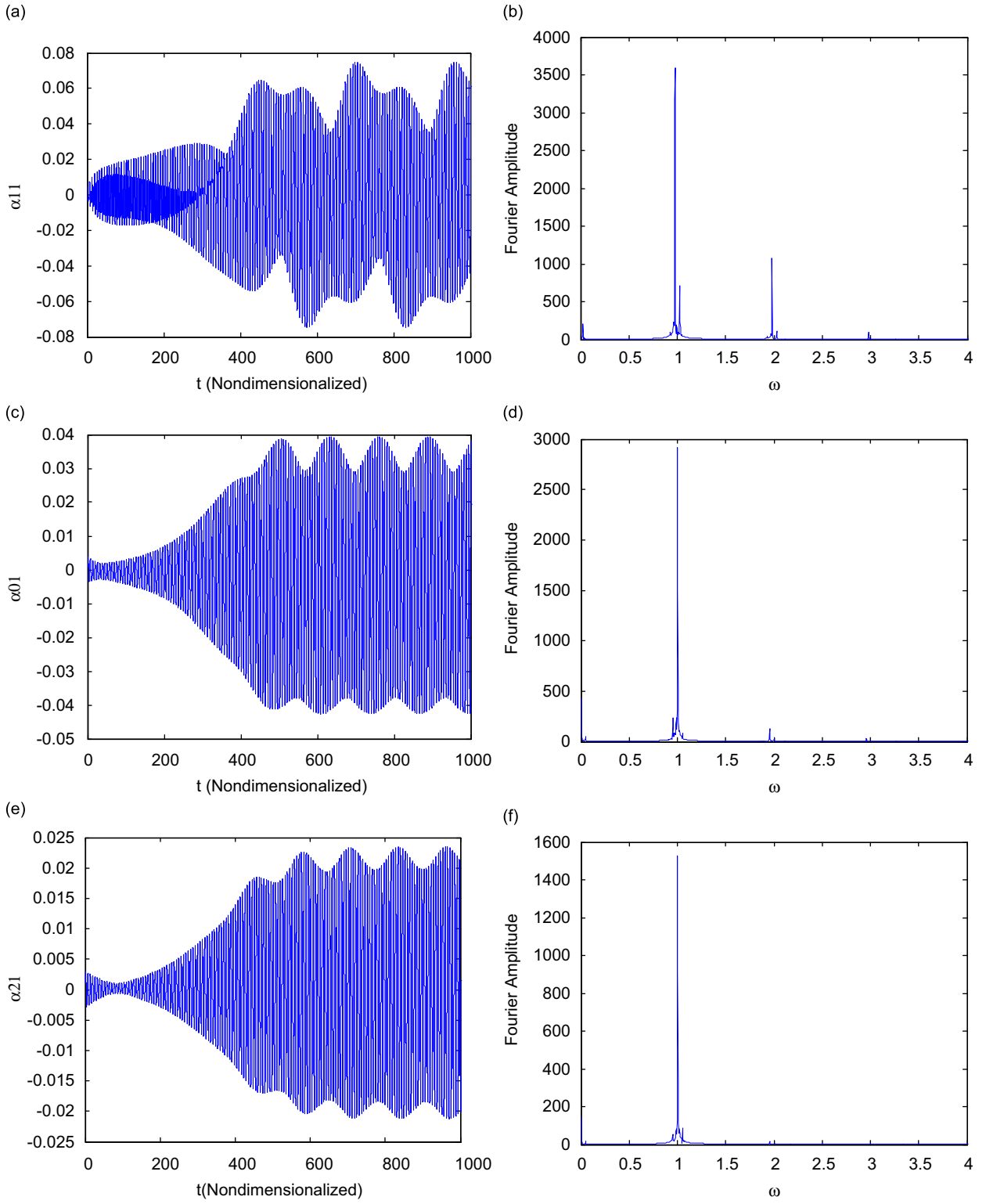

Fig. 8. Liquid modal amplitude for harmonic excitation at 1:2 resonance, $h/R = 0.5$, $m_L = 0.1$ M: (a) α_{11}, liquid first asymmetric modal amplitude, (b) Fourier amplitude of α_{11}, (c) α_{01}, liquid (0,1) modal amplitude, (d) Fourier amplitude of α_{01}, (e) α_{21}, liquid (2,1) modal amplitude, and (f) Fourier amplitude of α_{21}.

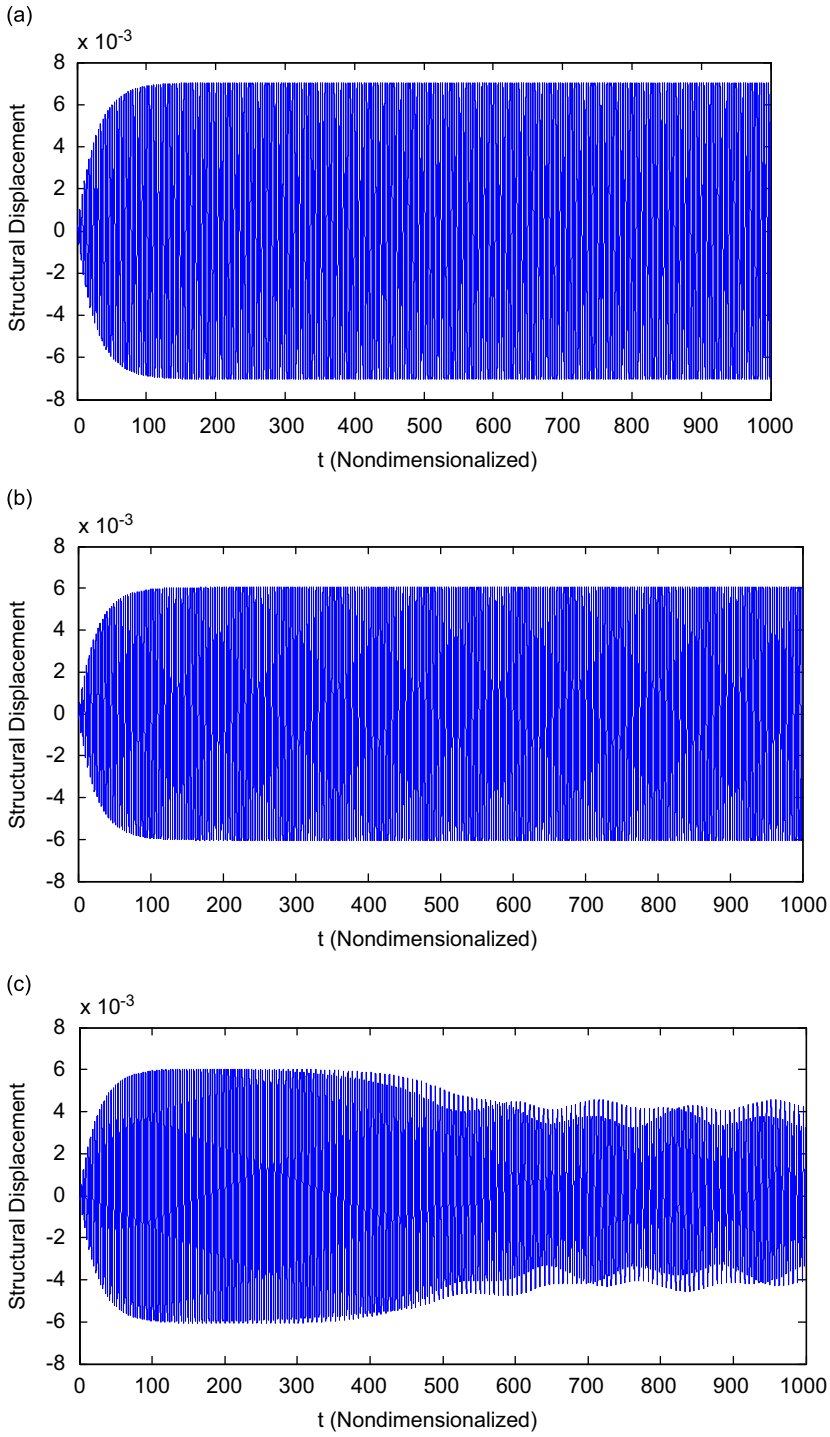

Fig. 9. Structural displacement for harmonic excitation at 1:2 resonance, $h/R = 1$, $m_L = 0.1$ M: (a) SDOF system, (b) structure with liquid tank—1 sloshing mode, and (c) structure with liquid tank—3 sloshing modes.

6.3. Earthquake excitation (resonance case 1:1)

All previous cases are considered in this example. The El-Centro earthquake excitation is used as an input to the system for the resonance case of $\omega_{11} = \omega_s$. The dominant frequency of the earthquake record was tuned to

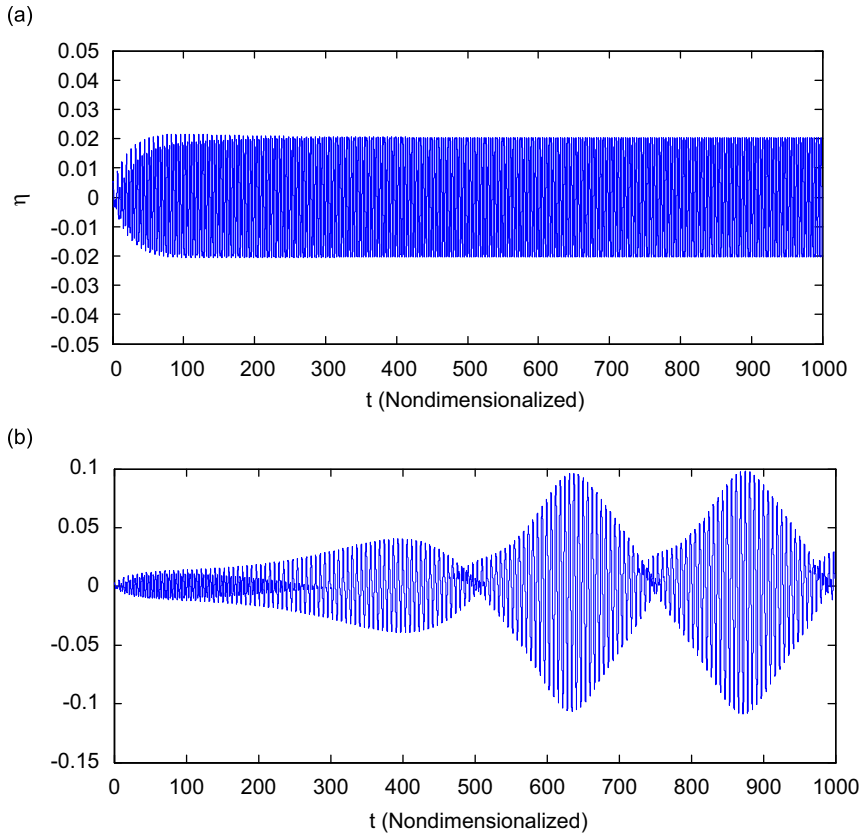

Fig. 10. Wave amplitude η for harmonic excitation at 1:2 resonance, $h/R = 1$, $m_L = 0.1\,\mathrm{M}$: (a) structure with liquid tank—1 sloshing mode and (b) structure with liquid tank—3 sloshing modes.

Table 3
El-Centro earthquake excitation, resonance case 1:1 ($\omega_{11} = \omega_s$)

Structural model		Maximum response[a]					Reduction (%)[b]	Approximation (%)[c]		
		x	η	α_{11}	α_{01}	α_{21}		x	η	α_{11}
$h/R = 1$	Structure with tank considering 3 sloshing modes	0.0253	0.2083	0.2856	0.0936	0.0231	41	–	–	–
$m_L = 0.1\,\mathrm{M}$	Structure with tank considering 1 sloshing mode	0.0256	0.1915	0.329	–	–	40.2	1.2	8.1	15.2
$h/R = 0.5$	Structure with tank considering 3 sloshing modes	0.0254	0.1289	0.1797	0.0495	0.0108	40.7	–	–	–
$m_L = 0.1\,\mathrm{M}$	Structure with tank considering 1 sloshing mode	0.0256	0.1914	0.329	–	–	40	1	49	83
$h/R = 1$	Structure with tank considering 3 sloshing modes	0.0324	0.3852	0.4137	0.2507	0.4328	24.3	–	–	–
$m_L = 0.02\,\mathrm{M}$	Structure with tank considering 1 sloshing mode	0.0337	0.4458	0.7575	–	–	21.3	4	16	83
$h/R = 0.5$	Structure with tank considering 3 sloshing modes	0.031	0.2446	0.3397	0.2237	0.1862	27.6	–	–	–
$m_L = 0.02\,\mathrm{M}$	Structure with tank considering 1 sloshing mode	0.0282	0.296	0.5087	–	–	34.1	9	21	49.7
SDOF system		0.0428	–	–	–	–	–	–	–	–

[a]Results are provided for the nondimensionalized parameters.
[b]The reduction in the peak response of the structural model is determined with respect to the SDOF system.
[c]Approximation is determined with respect to the 3 modes sloshing model as the most accurate case.

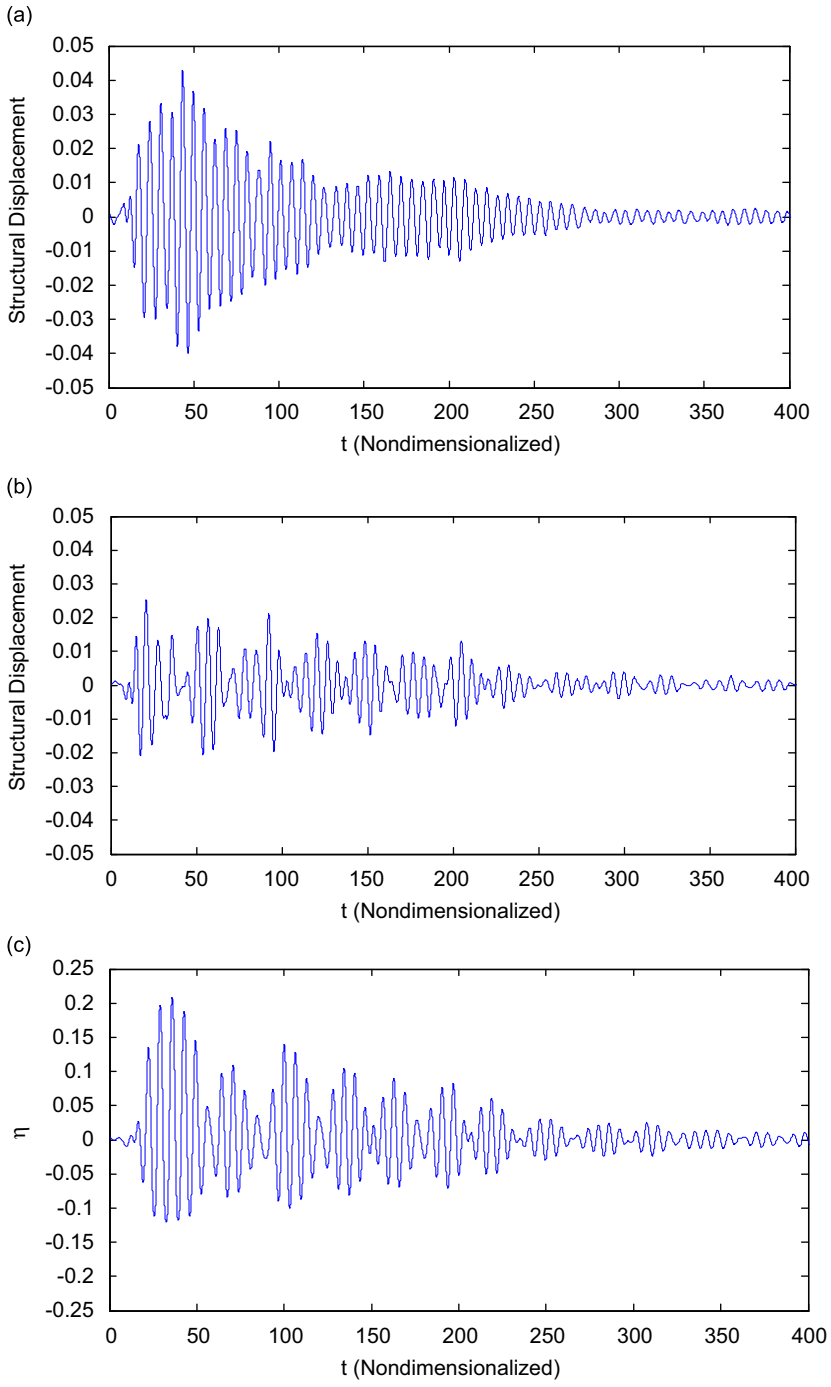

Fig. 11. El-Centro earthquake excitation at 1:1 resonance case, $h/R = 1$, $m_L = 0.1$ M: (a) structural displacement of SDOF system, (b) structural displacement of structure with liquid tank—3 sloshing modes, and (c) wave amplitude of structure with liquid tank—3 sloshing modes.

be near to the resonance frequency of the system through adjusting the time step intervals of the earthquake record. Table 3 shows the maximum response of the SDOF system alone and the system containing liquid tank with $h/R = 1$ and $m_L = 0.1$ M ratios. It seems that at the resonance case, 1:1, system efficiency even for

Table 4
El-Centro earthquake, excitation—resonance case 1:2 ($2B_4 = B_3$)

Structural model		Maximum response[a]					Reduction (%)[b]	Approximation (%)[c]		
		x	η	α_{11}	α_{01}	α_{21}		x	η	α_{11}
$h/R = 1$	Structure with tank considering 3 sloshing modes	0.0096	0.1169	0.1771	0.0469	0.0563	10.3	–	–	–
$m_L = 0.1\,\mathrm{M}$	Structure with tank considering 1 sloshing mode	0.0094	0.1017	0.1748	–	–	12.15	2.1	13	1.3
$h/R = 0.5$	Structure with tank considering 3 sloshing modes	0.01	0.0902	0.1339	0.0446	0.0245	6.6	–	–	–
$m_L = 0.1\,\mathrm{M}$	Structure with tank considering 1 sloshing mode	0.0101	0.0795	0.1366	–	–	5.6	1	11.9	2
$h/R = 1$	Structure with tank considering 3 sloshing modes	0.0094	0.1315	0.1774	0.0672	0.0902	12.2	–	–	–
$m_L = 0.02\,\mathrm{M}$	Structure with tank considering 1 sloshing mode	0.0094	0.1683	0.0979	–	–	12.2	0	25.5	5
$h/R = 0.5$	Structure with tank considering 3 sloshing modes	0.0094	0.0889	0.1359	0.0512	0.0369	12.15	–	–	–
$m_L = 0.02\,\mathrm{M}$	Structure with tank considering 1 sloshing mode	0.0095	0.075	0.1289	–	–	11.2	1.1	15.6	5.2
SDOF system		0.0107	–	–	–	–	–	–	–	–

[a]Results are provided for the nondimensionalized parameters.
[b]The reduction in the peak response of the structural model is determined with respect to the SDOF system.
[c]Approximation is determined with respect to the 3 modes sloshing model as the most accurate case.

earthquake excitation input is considerably improved in terms of maximum response reduction. The decreasing trend of response with respect to time is also acceptable in this case (Fig. 11).

6.4. Earthquake excitation (resonance case 1:2)

Table 4 shows the system's maximum response to the El-Centro earthquake excitation for the internal resonance case of $B_3 = 2B_4$ ($2\omega_{11} \approx \omega_s$). Also, the response time history of the SDOF system and the system with tank for $h/R = 1$ and $m_L = 0.1\,\mathrm{M}$ ratios are shown in Fig. 12. As this figure shows, in case of 1:2 resonance a large amount of energy is transferred from structure to liquid under the earthquake excitation. Also, one could observe the considerable frequency content of the structural response around the sloshing mode's frequency of the liquid.

7. Conclusion

The governing differential equations of motion of an elastic SDOF structural system carrying a liquid cylindrical tank are derived. These equations are numerically solved for the harmonic and earthquake excitation input at internal resonance cases 1:1 and 1:2. The response of system containing the liquid tank for 3 and 1 sloshing mode cases are compared with those for the case of SDOF system alone. A parametric study is carried out for different liquid mass m_L and h/R ratios. According to the obtained results, reducing h/R ratio and increasing m_L both will improve the performance of the liquid tanks in reducing the structural response caused by the external harmonic and earthquake excitations. On the other hand, it was shown that considering only 1 sloshing mode is not adequate for estimating the lateral structural response and maximum wave height. In the internal resonance case 1:2, for very large values of m_L, the system becomes unstable under external excitation frequencies near to the modal frequencies of the system. Also, for very small h/r ratios, traveling wave will be generated. Energy transfer from the structure to liquid and the shift in modal frequencies of the system are considered as the dominant factors in reducing the response of the system. As the Fourier

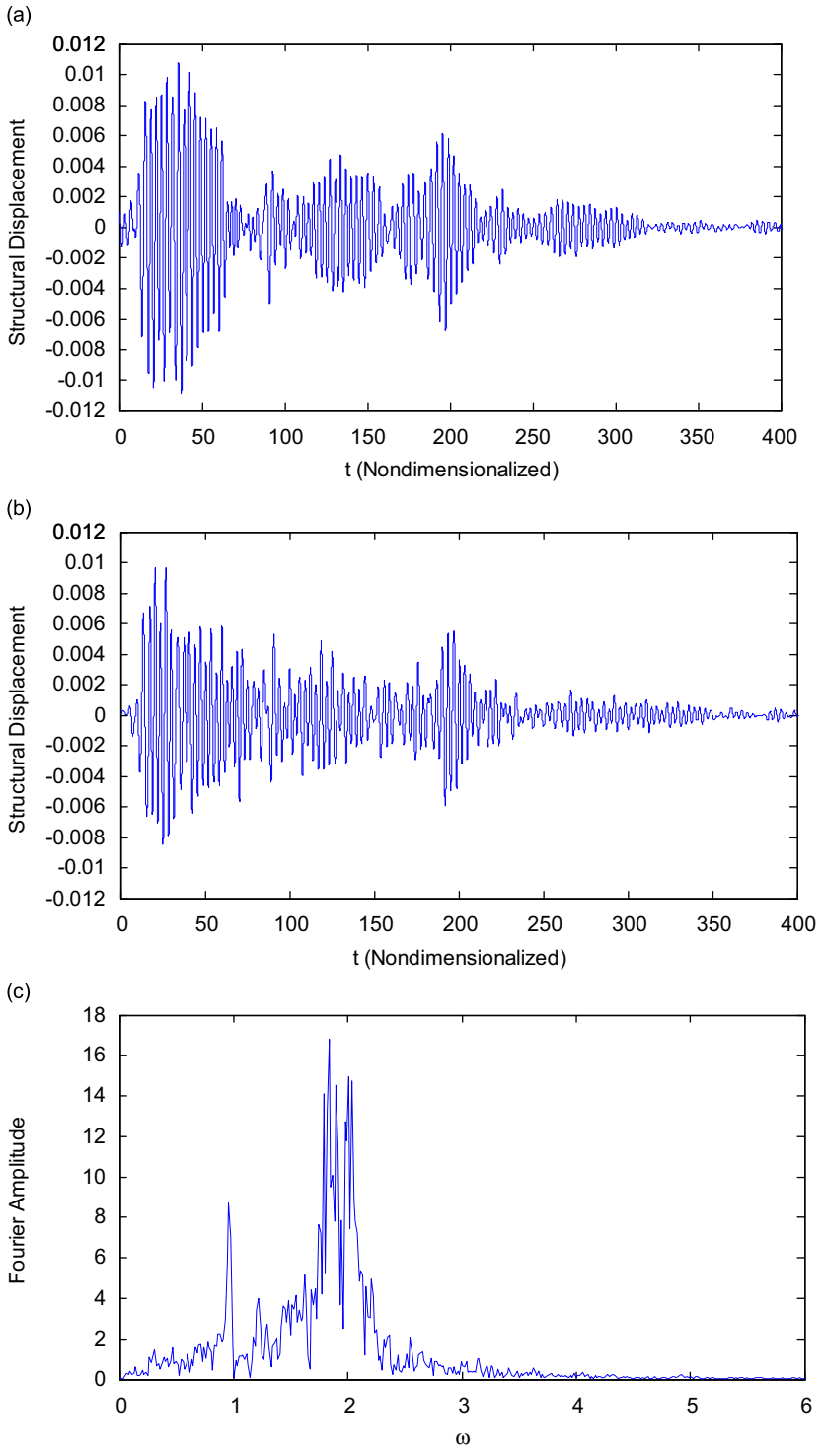

Fig. 12. El-Centro earthquake excitation at 1:2 resonance case, $h/R = 1$, $m_L = 0.1\,\mathrm{M}$: (a) structural displacement of SDOF system, (b) structural displacement of structure with liquid tank—3 sloshing modes, and (c) Fourier amplitude of structural displacement for structure with liquid tank—3 sloshing modes.

amplitude of the structural response indicates, even if the liquid is not excited directly, due to nonlinear interaction between the liquid and the structure, energy transfer from the structure to liquid would take place causing an increase in liquid's response while reducing the response of the structural system.

Appendix A

$$G_{m_1} = \int_0^1 rJ_m^2(\varepsilon_{m1}r)\,\mathrm{d}r, \quad g_{m1} = \int_0^1 1/rJ_m^2(\varepsilon_{m1}r)\,\mathrm{d}r$$

$$K_m^{ijk} = \frac{\int_0^1 rJ_0^i(\varepsilon_{01}r)J_1^j(\varepsilon_{11}r)J_2^k(\varepsilon_{21}r)\,\mathrm{d}r}{G_{m1}}, \quad U_m^{ijk} = \frac{\int_0^1 1/rJ_0^i(\varepsilon_{01}r)J_1^j(\varepsilon_{11}r)J_2^k(\varepsilon_{21}r)\,\mathrm{d}r}{G_{m1}}$$

$$\Gamma_m^{ijkl} = \frac{\int_0^1 rJ_i(\varepsilon_{i1}r)J_j(\varepsilon_{j1}r)\frac{\partial}{\partial r}[j_k(\varepsilon_k r)]\frac{\partial}{\partial r}[J_l(\varepsilon_{l1}r)]\,\mathrm{d}r}{G_{m1}}$$

$$\gamma_m^{ijk} = \frac{\int_0^1 rJ_i(\varepsilon_{i1}r)\frac{\partial}{\partial r}[J_j(\varepsilon_{j1}r)]\frac{\partial}{\partial r}[J_k(\varepsilon_{k1}r)]\,\mathrm{d}r}{G_{m1}}, \quad \psi_{mn} = \varepsilon_{mn}\tanh(\varepsilon_{mn}h), \quad \omega_{mn}^2 = \frac{\psi_{mn}}{\psi_{11}}$$

Appendix B

$$G_0 = \mu_1 + \mu_2\pi h, \quad G_1 = \frac{2}{(\varepsilon_{11}^2 - 1)J_1(\varepsilon_{11})}, \quad G_2 = \pi\mu_2\frac{J_1(\varepsilon_{11})\psi_{11}}{\varepsilon_{11}^2}$$

$$G_3 = \pi\mu_2\frac{\varepsilon_{01}\varepsilon_{11}}{\varepsilon_{01}^2 - \varepsilon_{11}^2}\left[(\psi_{01} - \psi_{11})\frac{\mathrm{d}J_1(\varepsilon_{11}r)}{\mathrm{d}r}\frac{\mathrm{d}J_0(\varepsilon_{01}r)}{\mathrm{d}r} + \left(\frac{\varepsilon_{01}^2\psi_{11} - \varepsilon_{11}^2\psi_{01}}{\varepsilon_{01}\varepsilon_{11}}\right)J_1(\varepsilon_{11}r)J_0(\varepsilon_{01}r)\right]$$

$$G_4 = \pi\mu_2\frac{\varepsilon_{11}\varepsilon_{21}}{\varepsilon_{11}^2 - \varepsilon_{21}^2}\left[\frac{1}{2}(\psi_{11} - \psi_{21})\frac{\mathrm{d}J_1(\varepsilon_{11}r)}{\mathrm{d}r}\frac{\mathrm{d}J_2(\varepsilon_{21}r)}{\mathrm{d}r} + (\psi_{11} - \psi_{21})J_1(\varepsilon_{11}r)J_2(\varepsilon_{21}r) + \frac{1}{2}\left(\frac{\varepsilon_{11}^2\psi_{21} - \varepsilon_{21}^2\psi_{11}}{\varepsilon_{11}\varepsilon_{21}}\right)J_1(\varepsilon_{11}r)J_2(\varepsilon_{21}r)\right]$$

$$G_5 = \frac{3\pi}{8}\mu_2 J_1^3(\varepsilon_{11}r)\psi_{11}, \quad G_6 = \frac{3\pi}{8}\mu_2\left[J_1^3(\varepsilon_{11}r)\left(\frac{1}{3} + \psi_{11}^2\right) + \varepsilon_{11}^2 J_1(\varepsilon_{11}r)\left(\frac{\mathrm{d}J_1(\varepsilon_{11}r)}{\mathrm{d}r}\right)^2\right]$$

$$Q_4 = \psi_{01}K_1^{120}, \quad Q_5 = \psi_{11}K_1^{120}, \quad Q_6 = \tfrac{1}{2}\psi_{11}K_1^{021}$$
$$Q_7 = \tfrac{1}{2}\psi_{21}K_1^{021}, \quad Q_8 = \tfrac{3}{8}\varepsilon_{11}^2K_1^{040}, \quad Q_9 = \gamma_1^{110}\varepsilon_{01}\varepsilon_{11} + K_1^{120}\psi_{01}\psi_{11}$$

$$Q_{10} = \tfrac{1}{2}\gamma_1^{112}\varepsilon_{11}\varepsilon_{21} + u_1^{021} + \tfrac{1}{2}K_1^{021}\psi_{11}\psi_{21}$$
$$Q_{11} = \tfrac{3}{4}\varepsilon_{11}^2\psi_{11}\Gamma_1^{1111} + \tfrac{1}{4}u_1^{040}\psi_{11} + \tfrac{3}{4}\varepsilon_{11}^2\psi_{11}K_1^{040}$$

$$Q_{12} = \tfrac{1}{2}\psi_{11}K_0^{120}, \quad Q_{13} = \tfrac{1}{4}\varepsilon_{11}^2\gamma_0^{011} + \tfrac{1}{4}u_0^{120} + \tfrac{1}{4}\psi_{11}^2K_0^{120}$$
$$Q_{14} = \tfrac{1}{2}\psi_{11}K_2^{021}, \quad Q_{15} = \tfrac{1}{4}\varepsilon_{11}^2\gamma_2^{211} - \tfrac{1}{4}u_2^{021} + \tfrac{1}{4}\psi_{11}^2K_2^{021}$$

$$Q_{16} = \gamma_1^{110}\varepsilon_{01}\varepsilon_{11} - \varepsilon_{01}^2K_1^{120}, \quad Q_{17} = \gamma_1^{110}\varepsilon_{01}\varepsilon_{11} - \varepsilon_{11}^2K_1^{120}$$
$$Q_{18} = \tfrac{1}{2}\gamma_1^{112}\varepsilon_{11}\varepsilon_{21} + u_1^{021} - \tfrac{1}{2}\varepsilon_{11}^2K_1^{021}, \quad Q_{19} = \tfrac{1}{2}\gamma_1^{112}\varepsilon_{11}\varepsilon_{21} + u_1^{021} - \tfrac{1}{2}\varepsilon_{21}^2K_1^{021}$$
$$Q_{20} = \tfrac{3}{4}\varepsilon_{11}^2\psi_{11}\Gamma_1^{1111} + \tfrac{1}{4}u_1^{040}\psi_{11} - \tfrac{3}{8}K_1^{040}\psi_{11}\varepsilon_{11}^2$$

$$Q_{21} = \tfrac{1}{2}\varepsilon_{11}^2\gamma_0^{011} - \tfrac{1}{2}\varepsilon_{11}^2K_0^{120} + \tfrac{1}{2}u_0^{120}, \quad Q_{22} = \tfrac{1}{2}\varepsilon_{11}^2\gamma_2^{211} - \tfrac{1}{2}\varepsilon_{11}^2K_2^{021} - \tfrac{1}{2}u_2^{021}$$

Appendix C

$$S_2 = \frac{Q_{16}}{\psi_{01}\psi_{11}}, \quad S_3 = \frac{Q_{19}}{\psi_{21}\psi_{11}}, \quad S_4 = \frac{Q_{16}}{\psi_{01}\psi_{11}}\left(\frac{Q_{16}Q_{21}}{\psi_{01}\psi_{11}} + \frac{Q_{19}Q_{22}}{\psi_{21}\psi_{11}}\right)$$

$$S_5 = \frac{Q_{19}}{\psi_{21}\psi_{11}}\left(\frac{Q_{16}Q_{21}}{\psi_{01}\psi_{11}} + \frac{Q_{19}Q_{22}}{\psi_{21}\psi_{11}}\right), \quad S_6 = \frac{1}{\psi_{11}}\left(\frac{Q_{16}Q_{21}}{\psi_{01}\psi_{11}} + \frac{Q_{19}Q_{22}}{\psi_{21}\psi_{11}}\right)$$

$$S_7 = \frac{Q_{17}}{\psi_{11}^2}, \quad S_8 = \frac{Q_{18}}{\psi_{11}^2}, \quad S_9 = \frac{Q_{20}}{\psi_{11}^2}$$

References

[1] C.C. Chang, M. Gu, Suppression of vortex-excited vibration of tall buildings using tuned liquid dampers, *Journal of Wind Engineering and Industrial Aerodynamics* 83 (1999) 225–237.

[2] K. Yamamoto, M. Kawahara, Structural oscillation control using tuned liquid damper, *Computers and Structures* 71 (1999) 435–446.

[3] V.J. Modi, S.R. Munshi, An efficient liquid sloshing damper for vibration control, *Journal of Fluids and Structures* 12 (1998) 1055–1071.

[4] Y. Fujino, L. Sun, B.M. Pacheco, P. Chaiseri, Tuned liquid damper (TLD) for suppressing horizontal motion of structure, *Journal of Engineering Mechanics* 118 (1992) 2017–2025.

[5] V.J. Modi, A. Akinturk, W. Tse, A family of efficient sloshing liquid dampers for suppression of wind-induced instabilities, *Journal of Vibration and Control* 9 (2003) 361–386.

[6] F. Rudinger, Tuned mass damper with fractional derivative damping, *Engineering Structures* 28 (2006) 1774–1779.

[7] R. Shepherd, The two mass representation of a water tower structure, *Journal of Sound and Vibration* 23 (1969) 391–396.

[8] R.A. Ibrahim, Autoparametric resonance in a structure containing a liquid, part I: two modes interaction, *Journal of Sound and Vibration* 42 (1975) 159–180.

[9] R.A. Ibrahim, A.D.S. Barr, Autoparametric resonance in a structure containing a liquid, part II, three modes interaction, *Journal of Sound and Vibration* 42 (1975) 181–200.

[10] R.A. Ibrahim, J.S. Gau, A. Soundararajan, Parametric and autoparametric vibrations of an elevated water tower part I, nonlinear parametric response, *Journal of Sound and Vibration* 121 (1988) 413–428.

[11] R.A. Ibrahim, W. LI, Parametric and autoparametric vibrations of an elevated water tower part II, autoparametric response, *Journal of Sound and Vibration* 121 (1988) 429–444.

[12] A. Soundararajan, R.A. Ibrahim, Parametric and autoparametric vibrations of an elevated water tower part III, random response, *Journal of Sound and Vibration* 121 (1988) 445–462.

[13] A.H. Nayfeh, *Nonlinear Interactions*, Wiley, New York, 2000.

[14] A.H. Nayfeh, P.F. Pai, *Linear and Nonlinear Structural Mechanics*, Wiley, New York, 2005.

[15] M. Amabili, M.P. Paidoussis, Review of studies on geometrically nonlinear vibrations and dynamics of circular cylindrical shells and panels, with and without fluid–structure interaction, *Applied Mechanics Reviews* 56 (2003) 349–381.

[16] M. Amabili, Nonlinear vibrations of circular cylindrical panels, *Journal of Sound and Vibration* 281 (2005) 509–535.

[17] M. Amabili, A. Sarkar, M.P. Paidoussis, Chaotic vibrations of circular cylindrical shells: Galerkin versus reduced-order models via the proper orthogonal decomposition method, *Journal of Sound and Vibration* 290 (2006) 736–762.

[18] J.W. Miles, Nonlinear surface wave in closed basins, *Journal of Fluid Mechanic* 75 (1976) 419–448.

[19] J.W. Miles, D. Henderson, Parametrically forced surface waves, *Annual Review of Fluid Mechanics* 22 (1990) 143–165.

[20] A.H. Nayfeh, R.A. Raouf, Nonlinear oscillation of circular cylindrical shells, *International Journal of Solids and Structures* 23 (1987) 1625–1638.

[21] T. Ikeda, R.A. Ibrahim, Random excitation of a structure interacting with liquid sloshing dynamics, *Proceedings of the ASME International Mechanical Engineering Congress & Exposition, New Orleans, LA*, 2002, pp. 1363–1374.

[22] V.N. Pilipchuk, R.A. Ibrahim, The dynamics of a nonlinear system simulating liquid sloshing impact in moving structures, *Journal of Sound and Vibration* 205 (1997) 593–615.

[23] T. Ikeda, N. Nakagawa, Nonlinear vibration of a structure caused by water sloshing in a rectangular tank, *Journal of Sound and Vibration* 201 (1997) 23–41.

[24] T. Ikeda, R.A. Ibrahim, Nonlinear random responses of a structure parametrically coupled with liquid sloshing in a cylindrical tank, *Journal of Sound and Vibration* 284 (2005) 75–102.

[25] T. Ikeda, S. Murakami, Autoparametric resonances in a structure/fluid interaction system carrying a cylindrical liquid tank, *Journal of Sound and Vibration* 285 (2005) 517–546.

[26] A.H. Nayfeh, J.F. Nayfeh, Surface waves in closed basins under principal and autoparametric resonance, *Physics of Fluids A: Fluid Dynamics* 2 (1990) 1635–1648.

[27] A.H. Nayfeh, Surface waves in closed basins under parametric and internal resonances, *Physics of Fluids* 30 (1987) 2976–2983.

[28] P. Holmes, Chaotic motion in weakly nonlinear model for surface waves, *Journal of Fluid Mechanic* 162 (1986) 365–388.
[29] A.H. Nayfeh, D.T. Mook, *Nonlinear Oscillation*, Wiley, New York, 1995.
[30] R.A. Ibrahim, *Liquid Sloshing Dynamic*, Cambridge University Press, Cambridge, UK, 2005.
[31] R.A. Ibrahim, V.N. Pilipchuk, T. Ikeda, Recent advances in liquid sloshing dynamics, *Applied Mechanics Reviews* 54 (2001) 133–199.
[32] V.V. Bolotin, *Dynamic Stability of Elastic Systems*, Holden Day Inc., San Francisco, 1964.